frontiers | Frontiers in Medicine

REVIEW
published: 28 June 2022
doi: 10.3389/fmed.2022.916693

ImmunoPET: Antibody-Based PET Imaging in Solid Tumors

*Reyhaneh Manafi-Farid[1], Bahar Ataeinia[2], Shaghayegh Ranjbar[3], Zahra Jamshidi Araghi[4], Mohammad Mobin Moradi[1], Christian Pirich[3] and Mohsen Beheshti[3]**

[1] Research Center for Nuclear Medicine, Shariati Hospital, Tehran University of Medical Sciences, Tehran, Iran, [2] Department of Radiology, Martinos Center for Biomedical Imaging, Massachusetts General Hospital and Harvard Medical School, Boston, MA, United States, [3] Division of Molecular Imaging and Theranostics, Department of Nuclear Medicine, University Hospital Salzburg, Paracelsus Medical University, Salzburg, Austria, [4] Rajaie Cardiovascular Medical and Research Center, Iran University of Medical Sciences, Tehran, Iran

Immuno-positron emission tomography (immunoPET) is a molecular imaging modality combining the high sensitivity of PET with the specific targeting ability of monoclonal antibodies. Various radioimmunotracers have been successfully developed to target a broad spectrum of molecules expressed by malignant cells or tumor microenvironments. Only a few are translated into clinical studies and barely into clinical practices. Some drawbacks include slow radioimmunotracer kinetics, high physiologic uptake in lymphoid organs, and heterogeneous activity in tumoral lesions. Measures are taken to overcome the disadvantages, and new tracers are being developed. In this review, we aim to mention the fundamental components of immunoPET imaging, explore the groundbreaking success achieved using this new technique, and review different radioimmunotracers employed in various solid tumors to elaborate on this relatively new imaging modality.

Keywords: immunoPET, monoclonal antibody (mAb), molecular imaging, solid tumors, immunoimaging, PET

OPEN ACCESS

Edited by:
Miguel Angel Morcillo, Medioambientales y Tecnológicas, Spain

Reviewed by:
Giorgio Treglia, Ente Ospedaliero Cantonale (EOC), Switzerland
Lurdes Gano, Centro de Ciências e Tecnologias Nucleares (C2TN), Portugal

****Correspondence:***
Mohsen Beheshti
m.beheshti@salk.at
orcid.org/0000-0003-3918-3812

Specialty section:
This article was submitted to Nuclear Medicine, a section of the journal Frontiers in Medicine

Received: *09 April 2022*
Accepted: *24 May 2022*
Published: *28 June 2022*

Citation:
Manafi-Farid R, Ataeinia B, Ranjbar S, Jamshidi Araghi Z, Moradi MM, Pirich C and Beheshti M (2022) ImmunoPET: Antibody-Based PET Imaging in Solid Tumors. Front. Med. 9:916693. doi: 10.3389/fmed.2022.916693

INTRODUCTION

There is an expanding insight into the role of different molecules and pathways in the development and progression of cancer. The growing knowledge about the involved molecules and processes has resulted in the modification in cancer management; therefore, targeted therapies and immunotherapies are increasingly utilized to treat different malignancies (1–3). This process was accelerated by the production of monoclonal antibodies (mAbs), following advances in DNA technology and Ab engineering (4). The targets can be membrane receptors, enzymes, or various molecules in signaling pathways, which are overexpressed or specifically present in a particular tumor or its microenvironment (5). Targeting molecules include Abs and Ab fragments, small molecule inhibitors, selective high-affinity ligands, some peptides, and aptamers (5, 6).

The first human radioimmunoimaging was conducted in 1978 using ^{131}I-labeled whole immunoglobin G (lgG) targeting carcinoembryonic antigen (CEA) (7) with inherent drawbacks. Since then, significant efforts have been implemented to develop ideal radioimmunoimaging tracers and radiopharmaceuticals for different cancers. The ideal tracer should be target-specific, biologically inert, highly stable in serum, minimally immunogenic, with rapid biodistribution and background clearance. Physiochemical characteristics to facilitate radiolabeling are also crucial (6, 8). For instance, manufactured small-sized Ab fragments (Fab) show higher specificity and rapid biodistribution and provide superior imaging characteristics over whole Abs (9, 10).

In the era of ever-growing targeted therapy, there is a requirement for accurate targeted imaging. Although immunohistochemistry (IHC) is the integral modality for detecting biomarkers (11), the non-invasive evaluation of the whole-body remains a compelling field of research, especially for patient selection and response evaluation. Medical imaging has a fundamental role in managing solid tumors, among which positron emission tomography (PET) is of particular importance (12). PET-based imaging demonstrates different functional and biochemical procedures occurring in normal tissues and malignant tumors at the cellular and molecular levels (12, 13).

The recent advances in PET acquisition systems, providing highly sensitive imaging (13), coupled with developments in labeling methods (14) and the specific targeting offered by mAbs, build the foundation of immunoPET. ImmunoPET is molecular imaging used for (1) the evaluation of biodistribution of Abs or their fragments in normal and malignant tissues, (2) the non-invasive detection of expression of target molecules and their heterogeneity in whole-body, and 3) prediction of response to targeted therapies (15). Although the concept of immunoPET is simple, it is an umbrella term covering almost all aspects of medical imaging, including oncology, infection/inflammation, neurological diseases, and drug development.

In this review, we aimed to provide a simplified summary of the current state of immunoPET in oncology. First, we briefly present the principles of immunoPET. Afterward, we focus on the Ab-based immunoPET in solid tumors and discuss the various developed probes in preclinical and clinical studies for each cancer.

THE CONCEPT OF IMMUNOPET

PET is a non-invasive and powerful imaging procedure with a wide range of clinical and research applications. PET provides the three-dimensional mapping of organs and lesions using a radioactive tracer. Radionuclides are incorporated either into compounds normally used by the organs, such as glucose, or into molecules that bind to receptors, peptides, cytokines, or other components of cellular pathways (16, 17). Recent advances in the development of PET systems and sophisticated software enable rapid, highly sensitive imaging (18). The combination of the superior targeting specificity of immune system-associated molecules and the inherent high sensitivity of PET technique establishes the principle of ImmunoPET (19). These tracers can specifically target various molecular pathways involved in the tumor biology (4).

Generally, the successful development of immunoPET in oncology is highly dependent on knowledge about the processes involved in tumor biology, choice of tumor-targeting vectors, radionuclides and chelators, and conjugation strategies. A vast number of molecules and processes are involved in tumor development and progression (20), the details of which are beyond the scope of this review. Some of the studied targets for imaging are discussed in more detail in the next section.

A variety of tumor-targeting vectors have been investigated for immunoPET. Full-length Abs are among the most used forms (21). Abs and associated amino acid-based macromolecules have been developed to display high specificity and binding affinity toward molecular targets overexpressed by cancer cells and tumor microenvironment (4). Their development dates back to the beginning of the twentieth century when Paul Ehrlich brought up the "magic bullet" idea to seek out and eradicate the spirochete of syphilis without affecting normal tissues (22).

MAbs are Abs with specificity for one particular epitope on an antigen (23). Despite the clinical success, these Abs come with a number of limitations including slow blood clearance, serum sickness, low target-to-background ratio (TBR), and the necessity of repetitive imaging (24). Moreover, high costs of production limit their use in developing countries. Thus, smaller Ab constructs have been engineered to overcome these limitations (25). Engineered Abs have a faster clearance rate, higher TBR, and are suggested to penetrate solid tumors more effectively (26).

Immunoglobulin G (IgG) is the most common type of Abs. IgG is composed of two main parts, crystallizable fragment (Fc) and antigen-binding Fragment (Fab), which contain polypeptides of heavy and light chains forming the constant and variable fragments of the IgG. The smaller fragments used for radiolabeling contain the variable domain. Fab and (Fab′)2 fragments are made by omitting the Fc region from Abs. They can have more rapid renal clearance and improved tumor penetration. However, their production is difficult and cannot be obtained from all subclasses of Abs (27). The smaller molecule, single-chain fragment variable (scFv), consists only of light and heavy variable chains. scFvs are produced more easily and are one of the most popular used fragments (28). The chains are attached with a non-covalent association, making scFv normally unstable. A disulfide bond between chains is used to increase stability, forming disulfide fragment variable (dsFv), and single-chain disulfide fragment variable (scdsFv). Proper tumor uptake and retention could be achieved by increasing the valency of scFvs molecules. Multivalent scFvs such as diabodies, tribodies and tetrabodies are favorable agents for radioimmunoimaging. In comparison with monovalent scFvs, tumor the retention time is augmented in multivalent scFvs. Also, their clearance time is shorter than whole Abs but equivalent to monovalent scFvs (25). scFvs are cleared through the urinary system, and there is significant retention in the kidneys (29).

Minibody is another engineered Ab fragment, produced by combining scFv molecule with human IgG1 constant heavy chain-3 (CH3) (30). Application of minibody is a mean to surmount slow renal clearance, which is the major problem of scFvs (29). Nanobodies or single-domain antibodies (sdAbs) are the smallest fragments of Abs obtained from the camelid heavy-chain-only Abs (31). Nanobodies are easier to produce and are more stable than scFvs (31). Finally, there is a smaller engineered targeting protein, affibody, which is derived from the IgG binding region. Affibodies seem to be a suitable protein for imaging but suffer from rapid clearance and decreased avidity to the targets (**Figure 1**) (27).

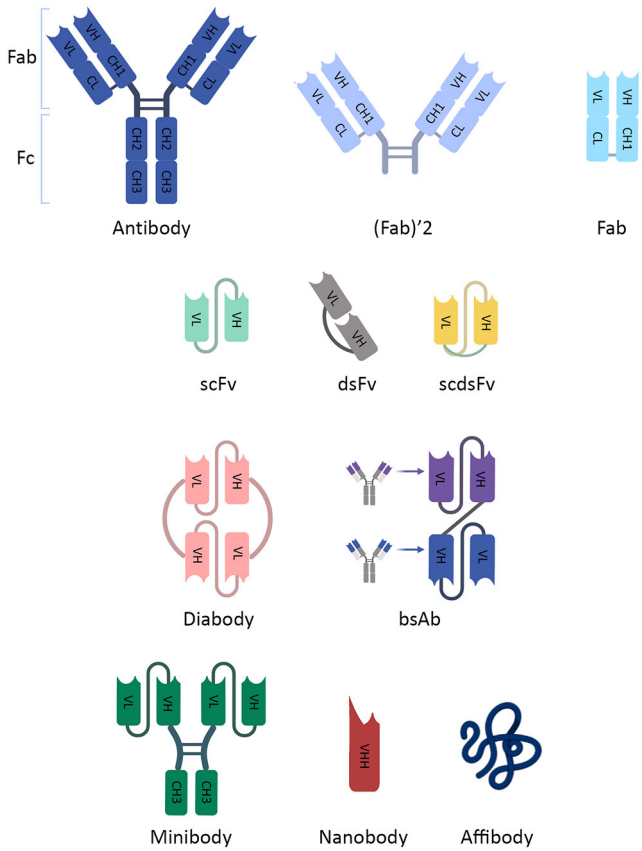

FIGURE 1 | The schematic illustration of an antibody and its fragments. The schematic illustration of an antibody and its fragments. IgG has two main parts, crystallizable Fragment (Fc) and antigen-binding Fragment (Fab). They contain fragments (constant [C] and variable [V]) which are composed of polypeptides of heavy (H) and light (L) chains. Due to inappropriate imaging characteristics, smaller fragments of Abs, which contain the variable domain for targeting, were developed. Fab and (Fab′)2 fragments are made by omitting the Fc region from Abs. scFv consists only of light and heavy variable chains. dsFv has a disulfide bond between chains, and scdsFv has both non-covalent and disulfide bonds to increase stability. scFv dimers (diabody) and multimers (not shown) provide more than one binding site. They can be multivalent scFvs containing different targeting fragments (bsAb). Minibody is an engineered Ab fragment, a combination of scFv with human IgG1 CH3. Nanobodies are the smallest fragment produced from natural heavy-chain-only Abs. CH, constant heavy chain; CL, constant light chain; dsFv, disulfide fragment variable; Fab, antibody fragment; Fc, crystallizable fragment; IgG, Immunoglobulin G; scdsFv, single-chain disulfide fragment variable; scFv, single-chain fragment variable; VH, variable heavy chain; VL, variable light chain; VHH, variable heavy chain of heavy-chain-only antibodies.

IMMUNOPET IN DIFFERENT MALIGNANCIES

ImmunoPET is known to provide excellent specificity and sensitivity in detecting some tumors (32, 33). However, some drawbacks include suboptimal imaging properties (feasibility, long imaging protocols), low expression of the targets in tumoral lesions, and high background activity in some organs.

Several molecules are involved in the development of different malignancies (**Table 1**). Receptor tyrosine kinases (RTKs) have been among the most explored targets for developing anticancer therapeutic and imaging agents. Substantial efforts have been made to establish immunoPET probes for revealing the heterogeneous expression of RTKs. The human epidermal growth factor (HER) family is one of the most evaluated RTKs, including four members, HER1-4 (101). A number of mAbs and Ab fragments have been developed for preclinical and clinical studies targeting anti-epidermal growth factor receptor (EGFR, known as HER1) in various malignancies (101), HER2 mostly in breast cancer (102), and HER3 in different solid tumors (103–106). Other RTKs, such as vascular endothelial-derived growth factor/receptor (VEGF/VEGFR) (107) and platelet-derived growth factor/receptor (PDGF/PDGFR) (82), and insulin-like growth factor-1 receptor (IGF-1R) (74) have also been targeted for immunoPET imaging.

Processes other than only high Ag-Ab affinity are required for appropriate targeting. The heterogeneous tracer uptake and high physiologic activity, especially in the liver and lymphoid tissue, can make imaging with these probes challenging (15, 106, 108). Preinjection of the cold tracer might decrease the hepatic uptake (109). Also, long radioimmunotracer clearance time for whole Abs can limit the tumor visualization (67, 110, 111). On the other hand, the renal retention of the smaller fragments is higher (112–115). Moreover, the poor vascular permeability of the tumors rather than the unfavorable characteristics of the probe can affect the outcome (17, 116).

The binding of programmed cell death protein ligand-1 (PD-L1) on the tumor cells to PD-1 on T-cells suppresses T-cell function and helps tumors escape the immune system. Immune checkpoint inhibitors (ICIs) are Abs that block PD-L1 and show therapeutic effect in various malignancies (117). Several radiolabeled ICIs have been developed for immunoPET, showing high physiologic uptake in lymphoid tissues (118, 119). Preinjection of unlabeled anti-PD-L1 may be useful for the PD-L1 expression evaluation (120). Also, T-cells in the tumor microenvironment impact response to therapies (121, 122) that have been evaluated in different malignancies (123–126), which can be used as a biomarker for response evaluation.

Many other proteins and molecules are overexpressed in different tumors, making them potential targets for immunoPET imaging. Some molecules and pathways are engaged in the development of various malignancies, and some are particularly found in distinct tumors. Below, we review the relevant evaluated probes in different malignancies.

Breast Cancer

Breast cancer is a heterogeneous malignancy with different features and outcomes (127). HER2 is a well-known prognostic biomarker and an effective therapeutic target (127, 128). Despite multiple therapeutic agents (127, 129), there is an unmet need to identify the patients who may benefit from these expensive and potentially toxic pharmaceuticals (109). There is intrapatient and intratumoral heterogeneity in expression of HER2 (15, 109, 130, 131), which is also dynamic over the disease course (129). This impacts the therapy response and the treatment

TABLE 1 | Biomarkers targeted in different malignancies for immunoPET imaging.

Biomarker	Type	Role
A33 (34)	Transmembrane glycoprotein	Interacts in cell adhesion.
ACKR3 (35)	Transmembrane protein	Interacts in cell adhesion, angiogenesis, tumor development and progression.
Axl (36)	Transmembrane RTK	Responsible for cancer development and progression Associated with survival.
CA 15-3 (MUC1) (37)	Transmembrane glycoproteins	Expressed on normal and malignant epithelial cells, possessing different functions (cell surface protection, cellular adhesion).
CA125 (MUC16) (38)	Transmembrane glycoproteins	Expressed on normal and malignant epithelial cells, possessing different functions (cell surface protection).
CA6 (39)	tumor-associated mucin 1-sialoglycotope antigen	Results of aberrant glycosylation in cancer cells.
CA-IX (40)	Cell surface protein	Overexpressed in hypoxia. Associated with tumor aggressiveness.
Cadherin-17 (CDH17) (41)	Transmembrane protein	Plays role in the adhesion of cells.
CD11b (42)	Transmembrane protein, a part of macrophage-1 antigen	Expressed on tumor-associated myeloid cells. Interacts in cell adhesion, migration, and complement 3 activation.
CD30 (43)	Transmembrane glycoprotein, member of TNF superfamily	Upregulated in T-cell activation. Regulates cytotoxic function of NK and T-cells.
CD38 (44)	A cell surface receptor and enzyme	Interacts in cell proliferation. May have role in resistance to ICIs.
CD44 (45)	A non-kinase transmembrane glycoprotein	Interacts in cell adhesion, migration, and metastasis. Responsible for cancer development and progression
CD44v6 (46)	An oncogenic variant of the cell surface molecule CD44	Responsible for cancer progression, invasion, and metastasis, overexpressed in squamous epithelium. Associated with resistance to therapy.
CD47 (47)	Transmembrane protein (macrophage immune checkpoint)	Plays role in the downregulation of immune response. Associated with poor prognosis.
CD133 (Prominin-1) (48)	Transmembrane glycoprotein	A stem cell identification marker. Associated with progression and poor prognosis.
CD146 (MUC18) (49, 50)	A cell surface protein	Interacts with VEGFR, activates epithelial-to-mesenchymal transition, which promotes metastatic potential and resistance to apoptosis. Associated with progression, invasion, and metastasis.
CD147 (51)	transmembrane protein of Ig superfamily	Inducts MMPs and VEGF expression. Associated with tumor growth and metastasis.
CDCP1 (52)	Transmembrane receptor	Regulates signaling pathways in tumors. Relays cancer promotion and associated with poor prognosis.
CEA (53–55)	Cell surface glycoprotein	Modulates intercellular adhesion, promotes cellular aggregation, and mediates transduction. Correlates with poorer survival. Enhances the potential of metastasis.
CTLA-4 (CD152) (56)	A membrane protein (Immune check point)	Plays role in the downregulation of immune response.
CXCR4 (57)	Transmembrane receptor for the chemokine CXCL12	Plays role in chemotaxis and cell proliferation.
Dll4 (58)	A ligand of Notch family transmembrane receptors	Activates Notch signaling and improves vascular function in tumors. Associated with poor prognosis.
Disease-associated ECM protein (59)	ECM proteins	ECM plays role in invasion, prognosis, angiogenesis, and resistance to therapies.
Endoglin (CD105) (60)	Accessory receptor for TGF-β	Overexpressed in endothelial of tissues with angiogenesis. Associated with poorer prognosis.
EpCAM (CD326) (61)	glycoprotein	Interacts in cell adhesion, intercellular interaction and migration.
FAP-α (62)	Transmembrane serine protease	Interacts in multiple mechanisms involved in tumor proliferation invasion, progression and resistance to therapy. Associated with poor prognosis.
Gal-3 (63)	Galactoside-binding protein	Modulates cell growth. Associated with prognosis.
GITR (64)	Co-stimulatory molecule for T-cell	Differential immune T-cell response.
GPC3 (65)	Cell-surface protein	Regulates cell growth. Associated with poor prognosis.

(Continued)

TABLE 1 | Continued

Biomarker	Type	Role
GRP78 (66)	A heat shock protein	Induced by lack of glucose. Associated with poor prognosis.
HER1 (EGFR) (67)	Transmembrane RTK	Involved in signal transduction, responsible for transcription of various genes. Enhances tumor cell survival, proliferation, and differentiation. Related with resistance to treatment.
HER2 (CD340) (68)	Transmembrane RTK	Involved in signal transduction, responsible for transcription of various genes. Important role in the growth, progression, and metastasis.
HER3 (69)	Transmembrane RTK	Responsible for cancer development and progression. Associated with poor prognosis and resistance to therapy.
HGF (70)	Cytokine	A ligand for MET. Associated with tumor development, progression and therapy resistance.
hk2 (71)	trypsin-like enzyme	Enhances sperm motility. Released in blood when the prostate gland structure is compromised.
ICAM-1 (CD54) (72)	Transmembrane protein	Plays role in cell adhesion.
ICOS (CD278) (73)	Co-stimulatory molecule for T-cell	Differential immune T-cell response.
IGF-1 (74)	Transmembrane RTK	Plays role in the development of cancer, proliferation, apoptosis, angiogenesis, tumor invasion, resistance to therapy
Integrin αvβ6 (75)	Cell surface receptor	Interacts with cell adhesion. Plays role in progression.
L1CAM (76)	Transmembrane protein	Plays role in cell adhesion, proliferation, migration, and invasion.
LGR5 (77)	Transmembrane glycoprotein, a marker of stem cells	Incorporates in tumor growth, therapy, and likely recurrence. Associated with metastasis, resistance, and poor prognosis.
MET (70)	Transmembrane RTK	Receptor of HGF. Tumor development, progression and therapy resistance
MG7 (78)	Gastric cancer-specific antigen	Overexpressed in gastric cancer. Associated with poor prognosis.
MSLN (79)	Membrane-bound surface glycosylphosphatidylinositol	Help tumor peritoneal implantation, proliferation and survival
MT1-MMP (80)	Endopeptidases	Degradation of ECM helping cell migration. Associated with tumor progression and metastasis.
OX40 (CD134) (64)	Co-stimulatory molecule for T-cell	Differential immune T-cell response.
PD-1/L1 (CD274) (81)	Transmembrane protein (immune checkpoint)	Plays role in the downregulation of immune response. Associated with resistance to therapy.
PDGF/PDGFR (82)	Transmembrane RTK	Incorporates in tumor cell growth and angiogenesis.
Syndecan-1 (CD138) (83)	Transmembrane cell-surface heparan sulfate proteoglycans	Affects several steps in tumor progression and facilitate metastasis. Correlates with poor prognosis and an aggressive phenotype.
Periostin (84)	ECM protein	Plays role in adhesion and motility in tumor microenvironment
peroxiredoxin-I (85)	Cell surface receptor	Plays role in oxidative stress. Prognostic factor for lung cancer.
PSA (86)	Kallikrein-like serine protease	Enhances sperm motility. Released in blood when the prostate gland.
PSCA (87)	cell surface protein	Overexpressed in prostate cancer. Plays role in signal transduction. Correlates with progression, metastasis and poor prognosis.
PSMA (88)	A transmembrane glycoprotein	Overexpressed in prostate cancer. Increases aggressiveness of prostate cancer.
RAGE (89)	Transmembrane receptor	Binding to multiple ligands. Plays role in transition to cancer.
RANKL (90)	A member of TNF	Plays role in osteoclastogenesis and bone Homeostasis. Plays resistance to immunotherapy.
TAG-72 (91)	Membrane-bound glycoprotein	A glycoprotein with mucin properties, overexpressed in some adenocarcinomas. Associated with progression.
TAM (92)	Macrophage	Associated with metastasis and poor response different therapies. Associated with poor survival.
TF (CD142) (93)	Transmembrane glycoprotein receptor	Initiates of the coagulation cascade.

(Continued)

TABLE 1 | Continued

Biomarker	Type	Role
TfR (94)	Transmembrane glycoprotein	Involves in iron uptake and cell growth.
TGF-β (95)	Cytokine	Plays a significant role cell proliferation, differentiation and apoptosis. Associated with poorer prognosis
TIL (96)	Lymphocyte	Responsible for malignant cells' death. The presence of TIL correlates with survival.
TIM-3 (97)	Immune checkpoint	Plays role in the downregulation of immune response.
TRA-1-60 (98)	Cell-surface antigen, a biomarker of stem cell	Associated with drug resistance and recurrence.
TROP-2 (99)	Transmembrane glycoprotein	Possesses stem-cell like qualities. Regulates proliferation, transformation and progression.
VEGF/VEGFR (100)	Transmembrane RTK	Responsible for tumor angiogenesis. Associated with progression and poor prognosis.

ACKR3, Atypical chemokine receptor 3, known as C-X-C chemokine receptor type 7; CA 15-3, Carcinoma antigen 15-3; CA125, Carbohydrate antigen 19-9; CA6, Carbonic anhydrase 6; CA-IX, Carbonic anhydrase-IX; CD, Cluster differentiation; CDCP1, CUB domain-containing protein 1; CEA, Carcinoembryonic antigen; CTLA-4, Cytotoxic T-lymphocyte associated protein-4; CXCR4, C-X-C chemokine receptor type 4; Dll4, Delta-like ligand 4; ECM, Extracellular matrix; EGFR, Epidermal growth factor receptor; EpCAM, Epithelial cellular adhesion molecule; EphA2, Ephrin receptor A2; FAP-α, Fibroblast activation protein-alpha; Gal-3, Galactoside-binding protein galectin-3; GITR, Glucocorticoid-induced tumor necrosis factor receptor; GPC3, Glypican-3; GRP78, Glucose-regulated protein; HER, Human epithelial receptor; HGF, Hepatocyte growth factor; hk2, Human kallikrein-related peptidase 2; ICAM-1, Intercellular adhesion molecule-1; ICI, Immune checkpoint inhibitor; ICOS, Inducible T-cell costimulatory receptor; IGF-1, Insulin-like growth factor-1; LGR5, Leucine-rich repeat-containing, G protein-coupled receptor 5; MMP, Matrix metalloproteinases; MSLN, Mesothelin; MT1-MMP, Membrane type-1 matrix metalloproteinases; MUC, Mucin; OX40, Tumor necrosis factor (ligand) superfamily, member 4; PD-1/PD-L1, Programmed cell death protein-1/ligand; PDGF/PDGFR, Platelet-derived growth factor/receptor; PSA, Prostate-specific antigen; PSMA, Prostate-specific membrane antigen; RAGE, Receptor for advanced glycation end products; RANKL, Receptor activator of nuclear factor kappa B ligand; RTK, Receptor tyrosine kinase; TAG-72, Tumor-associated glycoprotein-72; TAM, Tumor-associated macrophages; TF, Tissue factor; TfR, Transferrin receptor; TGF-β, Transforming growth factor beta; TIL, Tumor-infiltrating lymphocyte; TIM-3, T-cell immunoglobulin and mucin domain-containing-3; TNF, Tumor necrosis factor; TROP-2, Known as tumor-associated calcium signal transducer 2; VEGF/VEGFR, Vascular endothelial-derived growth factor/receptor.

options for patients. In this regard, several studies investigated radiolabeled mAbs and their fragments to develop new imaging agents targeting HER2. Proper tumor uptake and visualization of HER2-positive lesions were demonstrated using ^{89}Zr-labeled pertuzumab and trastuzumab in the preclinical (132, 133) and phase I clinical studies (102, 131, 134, 135).

Although new lesions were found (102), some HER2-positive lesions showed no significant uptake (102, 134), and the detection rate of 79–89% was reported (102, 134). Interestingly, HER2-targeting tracer uptake, suggesting HER2-positivity, was demonstrated in metastases from HER2-negative primary tumors (130, 131). The heterogenicity was also illustrated in metabolism on [^{18}F]FluoroDeoxyGlucose PET/computed tomography ([^{18}F]FDG PET/CT), with a discrepancy in the same-lesion standardized uptake value (SUV) between [^{18}F]FDG and [^{64}Cu]Cu-trastuzumab in HER2-positive lesions (109). This observation suggests a complementary role for both scans, further evaluated in a multicenter study (15). Gebhart et al. showed that pre-treatment [^{89}Zr]Zr-trastuzumab PET/CT accompanied by early metabolic response assessment using [^{18}F]FDG PET/CT best predicts the outcome after trastuzumab therapy (15). Moreover, to guide the treatment approach, [^{89}Zr]Zr-trastuzumab PET/CT increased physicians' confidence or altered management in a substantial ratio of patients (136). Also, early changes in [^{89}Zr]Zr-trastuzumab uptake correlated with response to therapy with a new experimental agent (137). The liver uptake is substantial with whole Abs, which may be decreased by the cold pharmaceutical preinjection (109).

To improve pharmacokinetics, scholars developed different HER2-targeting small Ab fragments in preclinical studies (138–141). Also, to enable early imaging and feasibility of labeling with more accessible radionuclides, such as ^{68}Ga, promising Ab fragments are investigated in early phase clinical studies (112–115, 142), showing a high correlation between the probe uptake, [^{68}Ga]Ga-ABY-025, and pathology (142). Expectedly, the renal retention is higher using Ab fragments (112–115).

Regulation of the immune system by ICIs have shown therapeutic efficacy in triple-negative breast cancer (143). Evaluating PD-L1 expression, Bensch et al. reported a heterogeneous tracer uptake in a few cancer types, including triple-negative breast cancer (144). The intensity of [^{89}Zr]Zr-atezolizumab (anti-PD-L1) uptake best correlated with outcome compared to IHC in their study (144). Currently, the role of [^{89}Zr]Zr-atezolizumab PET/CT is being investigated for patient selection for ICIs therapy (NCT02478099 and NCT02453984). Moreover, [^{89}Zr]Zr-Avelumab, another anti-PD-L1 ligand, is developed for the imaging of breast cancer in preclinical studies (145, 146).

In addition, CEA is a cell surface adhesion molecule (53), correlating with poor survival in breast cancer (54). Imaging with anti-CEA immunoPET seems promising. TF2 is a bispecific trivalent mAb comprising two humanized anti-CEA and an antihistamine-succinyl-glycine (HSG) hapten Fab fragments. This unique structure enables TF2 to be used in pretargeted imaging of malignancies with CEA expression (147). It showed more bone metastases than conventional imaging (148, 149) and helped delineate the clinical target volume for stereotactic body radiotherapy in CEA-positive metastatic breast cancer (148).

Furthermore, markers of tumor anagenesis have been targeted for immunoPET, which can be used as response prediction biomarkers to anti-angiogenesis therapies (150). The anti-VEGF, [^{89}Zr]Zr-bevacizumab, localized almost all primary breast lesions

(25/26) but was limited in the detection of metastatic lymph nodes (4/10) (151). Also, the uptake of anti-endoglin (anti-cluster of differentiation [CD]105), an accessory receptor for transforming growth factor-β (TGF-β), was demonstrated in mice models (60, 152–155).

There are also other prognostic biomarkers which have been evaluated for the imaging of triple-negative breast cancer in preclinical studies, such as syndecan-1 (CD138) (83) and IGF-1 (74).

Lung Cancer

Non-small cell lung cancer (NSCLC) is also a heterogeneous malignancy (156). Radioimmunoimaging in lung cancer has been performed in preclinical and clinical studies for various purposes.

Guidelines recommend targeted therapies for treating NSCLC using anti-EGFR and anti-VEGF/R mAbs (157). Similar to other therapies, it is crucial to predict the response before or early during the treatment. Radiolabeled Abs targeting EGFR (such as panitumumab and cetuximab) (10, 158–160) and VEGF/VEGFR (bevacizumab and ramucirumab) (150, 161, 162) have shown increased uptake in tumoral cells, including NSCLC (163–165). In pilot clinical studies, the feasibility and safety of administration of [^{89}Zr]-cetuximab (111) and [^{89}Zr]Zr-bevacizumab (166) were demonstrated in patients with NSCLC, showing TBRs of 0.9–4.5 and 0.7–8.6 in tumoral lesions for [^{89}Zr]Zr-cetuximab and [^{89}Zr]Zr-bevacizumab, respectively (111, 166).

ICIs are also increasingly administered in NSCLC patients with expression of PD-1/PD-L1 (167–169). Scholars have developed radiolabeled-ICIs to non-invasively evaluate the expression of PD-1/PD-L1 (170–172) and cytotoxic T-lymphocyte associated protein-4 (CTLA-4) (56). In clinical studies, [^{89}Zr]Zr-nivolumab (anti-PD-1), [^{18}F]BMS-986192 (anti-PD-L1 adnectin) (118) and [^{89}Zr]Zr-pembrolizumab (anti-PD-1) (173) demonstrated heterogeneous uptake and delineation of lesions larger than 2cm in some patients. The tumor uptake was insignificantly higher in responders to the anti-PD-1 treatment (118, 173).

The presence of tumor-infiltrating lymphocytes (TILs) correlates with survival in different malignancies (96). Also, the amount of T-cell infiltration after immunotherapy in the tumor microenvironment impacts the response (121, 122). The non-invasive evaluation of these cells may predict response to immunomodulatory therapies. Probes have been developed to monitor TILs dynamics after therapy (123–126). In this regard, an anti-CD8 minibody, [^{89}Zr]Zr-IAB22M2C, showed a favorable biodistribution (174), and currently, it is under investigation in phase II clinical trial for different solid tumors (NCT03802123). Also, the presence of tumor-associated macrophages (TAMs), indicating poorer survival (92), CD30, a marker of T-cell activation (175), and inducible T-cell costimulatory receptor (ICOS), a costimulatory signaling molecule (73) have been assessed using immunoPET.

MET is an RTK, a receptor of hepatocyte growth factor (HGF), which plays a role in the development, progression, and therapy resistance (70). ImmunoPET shows potential in the non-invasive evaluation of MET expression (176, 177). Another biomarker, CD146, interacts with VEGFR (17). It is overexpressed in about 50% of lung cancers and correlates with poor survival (178, 179). The [^{64}Cu]Cu-YY146 mAb showed a positive correlation with CD146 expression (49) and strong binding to CD146-expressing cell lines (50). Daratumumab (anti-CD38 mAb) is approved for treating multiple myeloma and is being investigated in a phase I/II clinical trial (NCT03665155). CD38 may have a role in resistance to immunotherapies (44). [^{89}Zr]Zr-daratumumab uptake has been reported in the CD38-expressing lung cancer model (44). Other probes against RTK [HER2 (180) and Axl (36)] and peroxiredoxin-I, a marker of oxidative stress (85), have also been assessed in NSCLC.

Colorectal Cancer

Tumor biomarkers are being investigated in metastatic colorectal cancer and are used to guide patient selection due to variable responses to available targeted therapies (181, 182).

Anti-EGFR therapy is used for Kirsten rat sarcoma virus (KRAS) wild-type tumors; however, not all patients respond to this therapy (183, 184). Anti-EGFR immunoPET using cetuximab and panitumumab showed specific but heterogeneous uptake in EGFR-expressing preclinical models (67, 160, 185, 186) and colorectal cancer patients (184). Evaluating the clinical impact in patient selection for therapy, van-Helden et al. failed to demonstrate a relation between [^{89}Zr]Zr-cetuximab-positivity and treatment response or outcome (183). Also, the high liver sequestration of [^{89}Zr]Zr-cetuximab in normal liver tissue is vital in colorectal cancer, limiting its diagnostic ability in liver metastasis (108).

Anti-CEA Ab scintigraphy was used for the first human radioimmunoimaging (7), and it is a relevant target for immunoPET (55). Different mAb and small Ab fragments have been developed for preclinical studies (187–189). However, pretargeted imaging using bispecific Ab (bsAb) seems more promising. Bispecific tracers (anti-CEA × anti-HSG) demonstrated highly specific tumor localization (190–193) and may outperform [^{18}F]FDG PET/CT (194). A recent phase I trial depicted the safety and feasibility of [^{68}Ga]Ga-IMP288 PET/CT (an anti-CEA × anti-HSG) with TF2 pretargeting, showing encouraging diagnostic performance for the detection of colorectal cancer metastases with the sensitivity of 88% and specificity of 100% (195).

T-cell redirecting bsAb are novel agents that target different antigens on T-cells and tumor cells, facilitating T-cell antitumor response (196). Using bsAbs, an anti-CEA × anti-CD3 [[^{89}Zr]Zr-AMG 211 (197)], and an anti-CEA × anti-interleukin-2 [[^{89}Zr]Zr-CEA-IL2v (198)] showed specific uptake in CEA-positive tumors, highlighting the potential value of such probes in immunomodulatory therapy response monitoring.

A33 is a glycoprotein responsible for cell adhesion, overexpressed in 95% of colorectal cancers (34). [^{124}I]I-huA33 PET/CT localized tumoral lesions in colorectal cancer patients (34, 199); however, the tracer uptake was also seen in normal bowel (34). To improve pharmacokinetics, pretargeted imaging was also evaluated, producing high-quality images in the preclinical studies (200, 201). The expression of another prognostic cell adhesion glycoprotein, CD44, was also

demonstrated in colorectal cancer models (202, 203). Tumor-associated glycoprotein-72 (TAG-72) was also targeted (204), which is a prognostic cell membrane molecule overexpressed in colorectal cancer with mucin (MUC) properties.

Moreover, the cancer stem cell hypothesis suggests the possible role of cancer stem cells in the progression of malignancies. In this regard, a few molecules have successfully targeted stem cells in preclinical studies, such as CD133 (205) and LGR5 (leucine-rich repeat-containing, G protein-coupled receptor 5) (77, 206). Additionally, probes monitoring TILs in response to immunotherapy have been evaluated in colorectal cancer models (124, 125).

There are other factors involved in tumor development, progression, and poor prognosis in colorectal cancer, assessed as targets for immunoPET in preclinical studies for the detection of colorectal cancer cell lines, including HER3 (69), angiogenesis factors [VEGFR (161) and PDGFRβ (82)], and hypoxia (M75 targeting carbonic anhydrase-IX [CA-IX]) (40, 207).

Prostate Cancer

Ongoing studies are striving to improve imaging in prostate cancer. The prostate-specific membrane antigen (PSMA) is known as a suitable target for prostate cancer imaging and therapy (208, 209). Agents targeting PSMA are classified into three groups: Abs, aptamers, and PSMA inhibitors (210). Here, we discuss Abs against the PSMA molecule and other targets for immunoPET imaging of prostate cancer.

ProstaScint ([^{111}In]In-capromab-pentitide) was the first FDA-approved mAb-based imaging, employing a mAb against PSMA (7E11) to detect occult pelvic lymph node metastases and recurrence of prostate cancer (211, 212). However, the binding of 7E11 to the intracellular epitope of PSMA resulted in low sensitivity for detecting metastases (213). To overcome this limitation, extracellular-binding mAbs were developed, such as J591 (88), labeled with imaging and therapeutic radionuclides (214–216). In a clinical study, the humanized [^{89}Zr]Zr-J591 (huJ591) showed accuracies of 60% and 95% for the detection of soft-tissue and bone metastases (217). However, mAbs have a prolonged circulation time due to their large size (218). In this regard, the third generation mAbs (minibodies/diabodies) were developed (219, 220). [^{89}Zr]Zr-IAB2M, a minibody, showed a favorable biodistribution (221) and promising diagnostic performance compared to magnetic resonance imaging (MRI) and [^{68}Ga]Ga-PSMA PET/CT (222). It had a sensitivity of 88% and a low specificity of 34% (222). Also, other anti-PSMA Abs, [^{64}Cu]Cu-3/A12 (223, 224), and [^{124}I]I-ScFvD2B (225), have successfully localized PSMA-positive prostate cancer xenografts.

One of the challenges in prostate cancer imaging is tumors with no or negligible PSMA uptake. Therefore, tracers targeting biomarkers of poorer prognosis may help detect or treat this subset of patients.

Various other Abs or Ab fragments have been evaluated in preclinical studies. Prostate stem cell antigen (PSCA) is a cell membrane protein that plays a part in signal transduction. Because of the slow kinetics of whole mAbs, different Ab fragments have been produced to target PSCA in preclinical studies (87, 226–228). It may become helpful in response evaluation to anti-androgen therapy (87). Low non-specific uptake has been reported with [^{124}I]I-A11 minibody (226) and slightly better with its smaller fragment, [^{89}Zr]Zr-A2cDb diabody (227, 229). Furthermore, TROP-2, known as tumor-associated calcium signal transducer 2, is a glycoprotein possessing stem-cell like qualities, overexpressed in some malignancies, (99). Pretargeted imaging with bsAbs, anti-TROP-2 × anti-HSG, may improve TBR and provide a fast, sensitive, and specific tool for prostate cancer imaging (218, 230). Also, a scFv against CD133, [^{89}Zr]Zr-HA10, localized in aggressive prostate cancer models (231, 232).

Others are anti-EpCAM Ab against epithelial cell adhesion molecule (233), [^{64}Cu]Cu-1A2G11 targeting IGF-1R (234), [^{89}Zr]Zr-Bstrongomab against TRA-1-60, an stem cell biomarker (98), [^{89}Zr]Zr-11B6 against androgen receptor-regulated human kallikrein-related peptidase 2 (71), and [^{89}Zr]Zr-5A10 against free prostate-specific antigen (235).

Prostate cancer cells have been targeted with different Abs and Ab fragments; however, few have been investigated in human studies. Mainly because PSMA inhibitors, showing favorable theranostic values (208, 209), have cast a shadow on other targets in prostate cancer. However, immunoPET may further help evaluate the aggressive variants (231, 232) or androgen receptor status or guide androgen receptor deprivation therapy (71). Also, it can have a role in radioimmunotherapy of patients who are not candidates or not responding to the currently available therapies.

Gastric Cancer

ImmunoPET has been investigated in gastric cancer only in limited studies. Targeted therapy against HER2 is recommended to treat gastric cancer with HER2-overexpression (168). ImmunoPET has shown promising results in the non-invasive evaluation of HER-positive lesions. Radiolabeled anti-HER2 (236, 237) and anti-HER3 (mAb3481) (238) successfully detected gastric cancer cells in mice models. Also, to assess therapy response after HER2-targeted therapy, a decrease in [^{89}Zr]Zr-trastuzumab uptake was demonstrated in the gastric cancer xenografts (239). Additionally, the dynamics of HER2 expression after pretreatment with lovastatin was evaluated using HER2 targeted immunoPET (240, 241). In initial clinical studies, [^{89}Zr]Zr-trastuzumab has shown a wide range of no to intense uptake in HER2-positive gastroesophageal cancers (242, 243). The uniformly high [^{89}Zr]Zr-trastuzumab uptake in all lesions was associated with a good response to therapy (243).

A few studies evaluated the MET/HGF pathway in gastric cancer. Radiolabeled rilotumumab (anti-HGF mAb) and onartuzumab (anti-MET mAb) non-invasively detected HGF and MET expression, respectively (244, 245). Additionally, MG7, a gastric cancer-specific antigen, is a prognostic biomarker (78). PET imaging of anti-MG7 Abs in gastric cancer xenografts showed a favorable binding affinity (246), but its application may be limited due to the overexpression of MG7 in helicobacter-related gastric disease (247). Also, radiolabeled anti-cadherin17 Ab (CDH17, an adhesion protein) was introduced as a potential probe for CDH17-positive gastric cancer (248).

Hepatocellular Carcinoma (HCC)

Imaging HCC, especially for lesions smaller than 2cm, is still challenging (249). There are only few studies that used immunoPET to evaluate HCC. Glypican-3 (GPC3) is a cell surface protein overexpressed in HCC (65). Different anti-GPC3 ^{89}Zr-labeled mAbs have been introduced, showing specific uptake in xenografts (250–252). To overcome the long biological half-life and weak tumor penetration, a F(ab$'$)2 fragment ([^{89}Zr]Zr-αGPC3-F(ab')2) was also developed (253). CD146 and CD38 are also expressed in HCCs. Imaging with an anti-CD146 dual-labeled tracer (^{89}Zr- and near-infrared fluorophore (NIRF), YY146-ZW8000), and an anti-CD38 ([^{64}Cu]Cu-daratumumab) showed specific tracer uptake in preclinical studies (254, 255).

Esophageal Cancer

ImmunoPET of esophageal cancer using multiple targets can provide useful information to detect primary tumors and metastases and identify tumor phenotype to facilitate patient selection for targeted therapies (57, 84, 256, 257).

Anti-EGFR imaging has been evaluated in a few preclinical studies, showing potential for [^{64}Cu]Cu-cetuximab PET/CT for the EGFR-expression detection and patient selection for cetuximab treatment (257, 258). Moreover, the detection of HER2 expression was evaluated in a small number of patients with gastroesophageal cancer (242). Similar to other malignancies, there was a wide range of uptake intensity from no uptake to SUV of 22.7 (242). Additionally, the decrease in vascular density after anti-VGEF treatment was depicted by [^{89}Zr]Zr-bevacizumab immunoPET (259). Finally, the overexpression of some biomarkers, such as periostin, an extracellular matrix (ECM) protein (84), and atypical chemokine receptor 3 (ACKR3), a cell adhesion transmembrane protein (35), was non-invasively depicted in esophageal cell lines.

Head and Neck Squamous Cell Carcinoma (HNSCC)

A few targets such as EGFR and CD44v6 have been evaluated in HNSCC (260, 261). Therapeutic Abs targeting EGFR showed promising outcomes in HNSCC treatment (262). Hence, ImmunoPET can be a valuable approach for diagnosis, treatment response prediction, and RIT planning in this group of cancers (46, 263–266). Several studies assessed the correlation of radiolabeled cetuximab uptake with EGFR expression to predict response to anti-EGFR therapies in HNSCC (67, 266–268), showing a clear tumor visualization in almost all patients (8/9) in phase I clinical trial (111). Similar to other malignancies, a mismatch of [^{89}Zr]Zr-cetuximab (67, 111, 268) and [^{64}Cu]Cu-panitumumab (116) uptake and EGFR expression was reported. However, an anti-EGFR affibody strongly correlated with EGFR expression alteration in response to cetuximab (269). Heat shock protein 90 (HSP90) is significantly associated with many oncoproteins and an interesting target for therapy (260). After HSP90 inhibitor therapy in a preclinical model, the amount of [^{124}I]I-cetuximab uptake was decreased in xenografts, but the uptake of [^{124}I]I-CD4v6 was unaffected (260). CD44v6 is a specific isomer of CD44, expressed in cells with squamous differentiation and overexpressed in squamous cell carcinomas in different organs (270). Preclinical studies on engineered anti-CD44v6 Abs, Ab fragments, and minibodies reported specific tumor uptake and more favorable kinetics in HNSCC animal models (46, 271, 272). In one of the first clinical studies,^{89}Zr-labeled anti-CD44v6, U36, detected primary tumors in all subjects and had equal performance to CT and MRI for the metastatic lymph node detection (273).

Thyroid Cancer

Thyroid cancer is a common malignancy, effectively managed with radioactive iodine. However, management of less common thyroid cancer subtypes is challenging. Recently, various molecules were evaluated for targeted imaging and therapy in these cancers (274, 275).

Expression of PDGFRα has been correlated with treatment resistance and risk of recurrence in papillary thyroid carcinoma (PTC). [^{64}Cu]Cu-D13C6, a PDGFRα targeting mAb, had specific uptake in PTC models, which can be of significant potential given that PTC is the most prevalent type of thyroid cancer (276). Moreover, β-galactoside-binding protein galectin-3 (Gal-3) is a biomarker, expressed only in thyroid cancer cells (63). ^{89}Zr-labeled targeting IgG and Fab fragments successfully detected thyroid cancer lesions and can potentially be used for identifying recurrence and metastasis (277–281).

Some anaplastic thyroid carcinomas (ATC) overexpress HER2. In this regard, dual-tracer imaging by ^{89}Zr- and IRDye 800CW-labeled pertuzumab depicted HER2-expressing ATC cell lines (282). Similar results were observed for an intercellular adhesion molecule-1 (ICAM-1), and tissue factor (TF or CD142, a mediator of hemostasis and inflammation) targeting probes in ATC models (72, 283). These findings can be of significant value in the diagnosis and management of this aggressive subtype. [^{124}I]I-U36, an anti-CD44v6, also demonstrated high ATC tumor accumulation independent of the iodine uptake (284).

Medullary thyroid carcinoma (MTC) is a rare subtype, significantly expressing CEA. The first clinical trial of pretargeted PET with TF2, a bispecific trivalent mAb of anti-CEA × anti-HSG, in relapsing MTC patients showed high tumor uptake (285). Moreover, the TF2 probe had superior sensitivity over [^{18}F]fluoro-l-dopa ([^{18}F]FDOPA) PET/CT (148, 286) and CT (286) in detecting metastatic lesions.

Pancreatic Cancer

Pancreatic ductal adenocarcinoma (PDAC) is the most common pancreatic malignancy (52). There is a need to improve the imaging modalities for the diagnosis and staging of PDAC (287, 288). Various Ab-based targets have been developed and are majorly evaluated only in preclinical studies, which may promote the role of immunoPET in PDAC (288).

Carbohydrate antigen 19-9 (CA 19-9), the known serum marker for PDAC, is detected on tumor cells in the vast majority of patients (289). Among agents targeting CA 19-9, a mAb, 5B1, demonstrated very high affinity and specificity (290), and immunoPET with [^{89}Zr]Zr-5B1 showed remarkable radiotracer uptake in the CA 19-9-positive models (291). Also, a dual-labeled tracer (^{89}Zr- and NIRF) successfully delineated tumoral lesions (292). It showed negligible non-specific uptake in CA

19-9-negative tumoral cell lines (292). However, the circulating CA 19-9 and long mAb half-life are problematic, increasing the background activity. In this regard, preinjection of cold 5B1 improved the image quality (293). Additionally, other pretargeting methods were assessed to overcome the drawbacks, including the development of a new-generation tracer (which exploits the advantages of reagents) (294) and an Ab-gold nanoparticle conjugate (295).

In the first clinical trial, [^{89}Zr]Zr-HuMab-5B1 PET/CT successfully detected the primary sites of PDACs, metastases, and small lymph nodes, overlooked by other imaging techniques (296). The tumor uptake was high, showing an average SUV of 19.7 ± 2.9, and the pretargeting increased TBR (296). Interestingly, serum CA 19-9 levels did not affect the physiologic distribution (296). Another ongoing phase I trial is assessing the performance of [^{89}Zr]Zr-HuMab-5B1 PET/CT in CA 19-9-positive tumors (NCT02687230).

Imaging with mAb was first conducted in PDAC using a murine Ab targeting MUC (297). Mucins are transmembrane glycoproteins highly expressed on several epithelial cancers, usually with an altered glycosylation pattern (37, 298). MUC1 or cancer antigen 15-3 (CA 15-3) may have a role in the management of PDAC (299). Also, carbohydrate antigen 125 (CA125), an extracellular domain of MUC16, is a well-known ovarian cancer biomarker (38). The newer generation of Abs targeted the unshed domain of MUC16 rather than CA125 and showed specific tracer uptake in PDAC xenografts with superior imaging characteristics (38).

Integrin αvβ6 is a cell surface protein, overexpression of which correlates with tumor progression (300) and seems as a potential theranostic agent in PDAC (301). However, the αvβ6-targeting peptides (302–304) are superior to Abs (300) and are more investigated.

Tissue factor (TF) is a transmembrane protein that plays a role in initiating coagulation and regulation of inflammation. The radiolabeled anti-TF, ALT-836, localized PDAC cell lines (93, 305). Additionally, a bsAb consisting of anti-TF × anti-endoglin improved binding affinity and localization of the xenografts (306, 307).

ECM proteins play a significant role in invasion, prognosis, angiogenesis, and resistance to therapies in some malignancies (59). Matrix metalloproteinases (MMPs) degrade ECM, helping cell migration. Abs targeting an ECM (59), a MMP protein (80), and a MMP inducer (CD147) (51) have localized PDAC in mice models.

Mesothelin (MSLN) is a membrane-bound glycoprotein overexpressed in more than 80–100% of pancreatic and ovarian cancer with an unknown specific role in tumor progression (108). MSLN-based immunoPET was previously used to evaluate the efficacy of MSLN-targeted antibody-drug conjugate (ADC) in preclinical models (308). In a clinical study on a small group of ovarian and pancreatic cancer patients, an ^{89}Zr-labeled anti-MSLN Ab detected the majority of malignant lesions with minimal non-specific uptake. Tumor tracer uptake also correlated with MSLN expression on IHC, but no correlation was observed with progression-free survival (309).

Indeed, many other probes have been assessed in only animal models, targeting RTKs [IGF-1R (310) and EGFR (311, 312)], PD-L1 (120), PSCA [A11 minibody (313) and a dual-tracer with ^{124}I and NIRF-A2cDb-800 (229)], TROP-2 (314), CEA (315, 316), ICAM-1 (317), and MET (318), as well as other less-evaluated radioimmunotracer against TRA-1-60 (98), CUB domain-containing protein 1 (CDCP1)(52), receptor for advanced glycation end products (RAGE) (319), glucose-regulated protein 78 (GRP78) (66), and transferrin receptor (TfR) (94).

Renal Cell Carcinoma (RCC)

CA-IX is a highly expressed membrane-bound antigen in RCC. Girentuximab is the chimeric version of G250, a mAb targeting CA-IX (320). Tumor uptake of radiolabeled G250 was established in preclinical and early clinical studies (321–324).

[^{124}I]I-girentuximab showed sensitivity and specificity of 86%, outperforming CT with 76% and 47%, respectively, in the REDECT clinical trial. However, performance declined for masses smaller than 2 cm (32, 33). ^{89}Zr revealed more favorable characteristics and substituted ^{124}I in further studies (325–327). [^{89}Zr]Zr-girentuximab PET/CT altered clinical management in various inconclusive diagnostic scenarios (328). Adding [^{89}Zr]Zr-girentuximab and [^{18}F]FDG PET/CT scans to CT improved lesion detection in metastatic RCC (329). High baseline SUV on [^{89}Zr]Zr-girentuximab also correlated with longer time to progression (330). Ongoing clinical trials will further elaborate on the diagnostic accuracy and theranostic potential of radiolabeled girentuximab (320, 331).

Furthermore, in preclinical studies, [^{89}Zr]Zr-atezolizumab localized PD-L1-positive RCC (332), and [^{64}Cu]Cu-bevacizumab reflected treatment response to everolimus, a mammalian target of rapamycin (mTOR) inhibitor (333). This finding was also observed in a clinical trial on everolimus in metastatic RCC; however, further clinical studies are required to confirm these findings (334).

Melanoma

The first trials of Ab-based imaging in melanoma date back to more than 25 years ago when Abs against the melanin-associated antigen (335) and a mouse monoclonal anti-melanoma Ab (336) were used for imaging in patients with metastatic malignant melanoma.

Currently, targeted therapies are the main systemic treatments for advanced melanoma (337, 338). It is crucial to document the presence of targets before the initiation of therapy to achieve the best response and avoid side effects (339, 340). Several preclinical studies showed favorable binding affinity and imaging of melanoma cell lines using Abs and Ab fragments targeting immune checkpoints, PD-1/PD-L1 (9, 119, 340–345) and CTLA-4 (346). However, the uptake in the lymphoid tissue was also high (119, 347). Moreover, radiotherapy-induced PD-L1 upregulation was demonstrated in melanoma mouse models, using radiolabeled anti-PD-L1 Abs (348, 349). Another immune checkpoint, T-cell immunoglobulin and mucin domain-containing-3 (TIM-3), was a successful target for murine

melanoma models (97). One clinical study evaluated [^{89}Zr]Zr-pembrolizumab in melanoma, reporting relations between tracer uptake and response to therapy and survival in patients with advanced or metastatic disease (347). Also, an ongoing phase II clinical trial is investigating the biodistribution and tumor uptake of [^{89}Zr]Zr-ipilimumab (anti-CTLA-4) in advanced melanoma (NCT03313323).

In addition to immune checkpoints, the number of CD4- and CD8-positive T-cells (121, 122) and the presence of costimulatory signaling molecules (64), namely OX40 (member 4 of tumor necrosis factor [TNF] family) and GITR (glucocorticoid-induced TNF Receptor), in the tumor microenvironment impact the response to immunotherapy. Preclinical studies using immunoPET probes successfully detected CD4- and CD8-positive rich tissues and upregulation of costimulatory substances (64, 122, 174, 350, 351). These probes have the potential to monitor immune response following different therapies. Moreover, immunoPET targeting ICAM-1 (72), CD146 (352), VEGF (353), and integrin-αvβ6 (75) was also successful in the detection of melanoma cells in preclinical studies.

Ovarian Cancer

Ovarian cancer comprises multiple subtypes and a diverse profile of overexpressed molecules (354). Moreover, the lack of effective specific treatment makes such molecules valuable for targeted therapies guided by immunoPET (108).

With the wide use of anti-HER2 mAbs, several studies evaluated ^{89}Zr/^{64}Cu-labeled anti-HER2 mAbs and their engineered fragments in preclinical models and compared different chelators and labeling strategies, or their optimal performance in vivo (138, 140, 355–361). Radiolabeled-trastuzumab has been used to monitor response not only to anti-HER2 mAbs but also to HSP90 inhibitors, which downregulate HER2 (361, 362). Using dual labeled mAbs combines pre-operative PET imaging and intra-operative optical imaging data. It can improve precise tumor and metastasis excision, especially in metastasis-prone tumors, such as ovarian cancer. Dual-labeled pertuzumab with ^{89}Zr and NIRF was used successfully for image-guided tumor resection in ovarian cancer xenografts (363).

Furthermore, VEGF imaging can be a response prediction biomarker to anti-angiogenesis therapies (150). [^{89}Zr]Zr-bevacizumab was a sensitive marker of early response to HSP90, mTOR, and VEGF inhibitors in ovarian cancer models (364–366).

CA125, an extracellular domain of MUC16, is a serological biomarker for treatment monitoring and recurrence of ovarian cancer (298). Preclinical studies on the ^{89}Zr/^{64}Cu-labeled oregovomab, an anti-CA125 mAb, reported high uptake in ovarian cancer xenografts (367, 368). Furthermore, [^{89}Zr]Zr-oregovomab detected histologically-confirmed lymph node involvement (368). The newer generation of Abs targeting MUC16 showed superior imaging characteristics (38, 369). Additionally, an ^{89}Zr-labeled anti-MUC1 or CA 15-3 also showed proper performance in vivo (37). The first clinical study on a Fab targeting carbonic anhydrase 6 (CA6) epitope of MUC1 reported the safety of this probe in an ovarian cancer patient, and the probe correctly reflected the low tumor expression of CA6 observed in IHC (370).

REGN4018, a T-cell engaging bsAb targeting MUC16 × CD3, is currently being investigated in a clinical trial for ovarian cancer (NCT03564340). It had high specific uptake in tumors and lymphoid organs in preclinical studies (371). [^{89}Zr]Zr-ERY974, a bsAb targeting CD3ε on T-cells × GPC3, showed high specific uptake in GPC3-positive ovarian cancer xenografts ingrafted with immune cells compared to xenografts in immunodeficient mice, highlighting the potential value of such probes in immunotherapy response monitoring (372).

Finally, as mentioned in the pancreatic cancer section, MSLN expression may be non-invasively evaluated in ovarian cancer, using ^{89}Zr-labeled anti-MSLN Ab (309), which may help patient selection for therapy.

Central Nervous System (CNS)

Precision imaging and targeted therapy in the central nervous system (CNS) is challenging due to the limited distribution of radiopharmaceuticals beyond the blood-brain barrier (BBB), especially for high molecular weight compounds such as Abs. However, disruption of BBB by tumors can lead to the appropriate probe uptake (373). Nanobodies are attractive probes for CNS malignancies given their small size, easy BBB penetration, and faster blood clearance (374). ImmunoPET has also been helpful to monitor brain drug delivery alteration in response to different methods of increasing BBB permeability (375–378) and predict response to intrathecal radioimmunotherapy (379).

Several studies, mainly preclinical, investigated radioimmunotracers targeting molecules involved in angiogenesis, such as VEGF (380, 381), CD146 (382, 383), and PDGFRβ (384) in the setting of brain tumors. On clinical studies of the mentioned targets, [^{89}Zr]Zr-bevacizumab imaging was feasible and safe in children with diffuse intrinsic pontine glioma; however, significant uptake heterogeneity was observed (385). Interestingly, high expression of PSMA by neovascular endothelium has been reported in a number of highly vascularized tumors, including gliomas and some brain metastases (386). This phenomenon makes PSMA a potential target to monitor response to anti-angiogenesis treatments in brain malignancies. Matsuda et al. showed high PSMA expression in histological specimens for a wide range of brain malignancies, including gliomas and metastatic brain lesions. Next, they successfully imaged three patients with recurrent glioma or brain metastasis with [^{89}Zr]Zr-IAB2M (387).

Additionally, the TGF-β is a known cytokine involved in the development of various malignancies (95). A radioimmunotracer targeting TGF-β, [^{89}Zr]Zr-fresolimumab, was successfully produced (388). In a clinical trial on high-grade glioma patients undergoing anti-TGF-β treatment, [^{89}Zr]Zr-fresolimumab accumulated in most tumors, except for some lesions smaller than 10 mm or those with radionecrosis (95).

Another group of glioma tracers evaluates immune system components in the tumor microenvironment by targeting immune cell infiltration and activation markers, such as CD8+ lymphocytes (389), its co-stimulatory molecule, OX40 (390), a

marker of tumor-associated myeloid cells, CD11b (391, 392), a phagocytosis checkpoint molecule, CD47 (393), and lymphocyte checkpoint molecule/ligand, PD-1/PD-L1 (378, 394).

Finally, immunoPET targeting other overexpressed biomarkers responsible for tumor development or progression are also under investigation in gliomas, including RTKs [ephrin receptor A2 (EphA2) (395) and EGFR (396–400)], stem cell marker, CD133 (401), fibroblast activation factor-alpha (FAP-α) (402), Delta-like ligand 4 (Dll4, which is a ligand for a membrane receptor in different signaling pathways) (58), HGF (244), and MMP (403).

Others

ImmunoPET studies on other malignancies are still in the preclinical setting. For instance, early murine studies targeting EGFR and CA 19-9 were promising in bladder cancer models (404, 405). An anti-CD3 probe also detected T-cell infiltration in bladder cancer-bearing mice, reflecting the potential for future studies on immunotherapy response prediction in urothelial cancers (406).

Evaluating mesothelioma, an anti-MSLN Ab, [^{89}Zr]Zr-amatuximab, detected MSLN-expressing xenografts (308, 407), which can play a part in the patient selection for anti-MSLN targeted therapy. EGFR is also overexpressed in mesotheliomas (408). In this regard, receptor-specific uptake of [^{86}Y]Y-cetuximab and [^{86}Y]Y-panitumumab were documented, showing more favorable tumor-targeting characteristics with the latter (158). Also, a radiolabeled anti-EGFR Ab that selectively targets an epitope of EGFR detected EGFR-expressing xenografts (408). In cholangiocarcinoma cell lines, L1CAM overexpression, a cell adhesion molecule, was depicted using [^{64}Cu]Cu-cA10-A3 probe (76, 409, 410). Recently, the role of receptor activator of nuclear factor-kappa B/ligand (RANK/RANKL) is recognized in resistance to immunotherapy. Its expression was non-invasively assessed by [^{89}Zr]Zr-denosumab in cervical and HNSCC xenografts (90). Finally, CD44v6 overexpression was documented in vulva cancer cell lines using an anti-CD44v6 minibody, using [^{124}I]I-AbD19384 (271).

CONCLUSION

In the era of precision medicine and molecular targeted therapy, the need for accurate targeted imaging is inevitable. Given the inherent favorable characteristics, immunoPET seems very promising in this regard. A broad spectrum of both tumor-specific and common general molecules in different malignancies has already become targets for radioimmunoimaging of cancer. However, only a few have been introduced in clinical studies (**Supplementary Table 1**). Some common obstacles to the wide implementation of immunoPET include the high costs, advanced technology to commercially produce pure mAbs, difficulties in conjugation and in vivo tracer stability, as well as high circulation time and physiologic uptake after administration. Recent developments are answering these needs (97, 411) and will continue to evolve. Although immunoPET can become a diagnostic tool in specific conditions, its primary role seems to be a complementary imaging tool for therapy guidance.

Almost all studies mention the heterogeneous uptake of probes in different tumors. That is where the immunoPET strength lies, i.e., non-invasively depicting the heterogeneity of tumoral lesions. ImmunoPET tracks target expression and pharmacokinetics of mAbs in vivo before and after certain treatments, pointing out its potential value for patient recruiting and response monitoring of targeted therapies. Noteworthy, smaller Ab fragments provide more favorable imaging properties that can help increase the detection rate and accuracy of the imaging. However, the implementation of whole Abs is crucial since these structures are used for treatment, and the goal is to demonstrate their in vivo distribution.

Another advantage of developing new radioimmunoimaging probes is the theranostic application. The probes can be labeled with positron-emitting imaging and beta/alpha-emitting therapeutic radiometals, providing another possible treatment option for different malignancies.

Besides developing new targeting probes, future studies should also focus on the predictive and prognostic value of the radioimmunotracers after targeted therapies to further elaborate on their impact on treatment selection.

AUTHOR CONTRIBUTIONS

RM-F, CP, and MB came up with the main study topic and designed the outline. RM-F and BA performed the initial search and screened the literature to finalize the topics to cover. RM-F, BA, SR, ZA, and MM performed the literature search and extracted and summarized the data. All authors contributed to writing the initial draft of the manuscript under the supervision of RM-F, CP, and MB. ZA, BA, and RM-F drafted the tables. RM-F and SR prepared the figure. BA proofread and edited the final version of the manuscript. All authors read and approved the final version prior to submission.

SUPPLEMENTARY MATERIAL

The Supplementary Material for this article can be found online at: https://www.frontiersin.org/articles/10.3389/fmed.2022.916693/full#supplementary-material

REFERENCES

1. Chen DS, Mellman I. Oncology meets immunology: the cancer-immunity cycle. *Immunity.* (2013) 39:1–10. doi: 10.1016/j.immuni.2013.07.012
2. Raval RR, Sharabi AB, Walker AJ, Drake CG, Sharma P. Tumor immunology and cancer immunotherapy: summary of the 2013 SITC primer. *J Immunother Cancer.* (2014) 2:14. doi: 10.1186/2051-1426-2-14
3. Bedard PL, Hyman DM, Davids MS, Siu LL. Small molecules, big impact: 20 years of targeted therapy in oncology. *Lancet.* (2020) 395:1078–88. doi: 10.1016/S0140-6736(20)30164-1
4. Harsini S, Alavi A, Rezaei N. Introduction on Nuclear Medicine and Immunology. *Nucl Med Immunol.* (2022) 22:1–13. doi: 10.1007/978-3-030-81261-4_1
5. Chakraborty D, Das A, Bal C. *Tumor-Targeting Agents. Nuclear Medicine and Immunology.* (New York, NY: Springer), p. 217–36 (2022).

6. Alam IS, Shaffer TM, Gambhir SS. *Nuclear Imaging of Endogenous Markers of Lymphocyte Response. Nuclear Medicine and Immunology* (New York, NY: Springer), p. 15–59 (2022).
7. Goldenberg DM, DeLand F, Kim E, Bennett S, Primus FJ, van Nagell JR. Jr., et al. Use of radiolabeled antibodies to carcinoembryonic antigen for the detection and localization of diverse cancers by external photoscanning. *N Engl J Med.* (1978) 298:1384–6. doi: 10.1056/NEJM197806222982503
8. Wu AM. Engineered antibodies for molecular imaging of cancer. *Methods.* (2014) 65:139–47. doi: 10.1016/j.ymeth.2013.09.015
9. McCarthy CE, White JM, Viola NT, Gibson HM. In vivo imaging technologies to monitor the immune system. *Front Immunol.* (2020) 11:1067. doi: 10.3389/fimmu.2020.01067
10. Wong KJ, Baidoo KE, Nayak TK, Garmestani K, Brechbiel MW, Milenic DE. In Vitro and In Vivo pre-clinical analysis of a F(ab')(2) fragment of panitumumab for molecular imaging and therapy of her1 positive cancers. *EJNMMI Res.* (2011) 1:1. doi: 10.1186/2191-219X-1-1
11. Sukswai N, Khoury JD. Immunohistochemistry innovations for diagnosis and tissue-based biomarker detection. *Curr Hematol Malig Rep.* (2019) 14:368–75. doi: 10.1007/s11899-019-00533-9
12. Reddy S, Robinson MK. Immuno-positron emission tomography in cancer models. *Semin Nucl Med.* (2010) 40:182–9. doi: 10.1053/j.semnuclmed.2009.12.004
13. James ML, Gambhir SS, A. molecular imaging primer: modalities, imaging agents, and applications. *Physiol Rev.* (2012) 92:897–965. doi: 10.1152/physrev.00049.2010
14. Morais M, Ma MT. Site-specific chelator-antibody conjugation for PET and SPECT imaging with radiometals. *Drug Discov Today Technol.* (2018) 30:91–104. doi: 10.1016/j.ddtec.2018.10.002
15. Gebhart G, Lamberts LE, Wimana Z, Garcia C, Emonts P, Ameye L, et al. Molecular imaging as a tool to investigate heterogeneity of advanced HER2-positive breast cancer and to predict patient outcome under trastuzumab emtansine (T-DM1): the ZEPHIR trial. *Ann Oncol.* (2016) 27:619–24. doi: 10.1093/annonc/mdv577
16. Lameka K, Farwell MD, Ichise M. Positron emission tomography. *Handb Clin Neurol.* (2016) 135:209–27. doi: 10.1016/B978-0-444-53485-9.00011-8
17. Wei W, Rosenkrans ZT, Liu J, Huang G, Luo QY, Cai W. ImmunoPET: Concept, design, and applications. *Chem Rev.* (2020) 120:3787–851. doi: 10.1021/acs.chemrev.9b00738
18. López-Mora DA, Carrió I. Advances and new indications of PET/CT SCAN. *Med Clin (Barc).* (2021) 156:65–7. doi: 10.1016/j.medcle.2020.04.027
19. Narayanaswami V, Dahl K, Bernard-Gauthier V, Josephson L, Cumming P, Vasdev N. Emerging PET radiotracers and targets for imaging of neuroinflammation in neurodegenerative diseases: outlook beyond TSPO. *Mol Imaging.* (2018) 17:1536012118792317. doi: 10.1177/1536012118792317
20. GM C. *The Cell: A Molecular Approach*. Sunderland (MA): Sinauer Associates (2000). Available fonline at: https://www.ncbi.nlm.nih.gov/books/NBK9963/.
21. Scott AM, Wolchok JD, Old LJ. Antibody therapy of cancer. *Nat Rev Cancer.* (2012) 12:278–87. doi: 10.1038/nrc3236
22. Pressman D, Keighley G. The zone of activity of antibodies as determined by the use of radioactive tracers; the zone of activity of nephritoxic antikidney serum. *J Immunol.* (1948) 59:141–6.
23. Köhler G, Milstein C. Continuous cultures of fused cells secreting antibody of predefined specificity. *Nature.* (1975) 256:495–7. doi: 10.1038/256495a0
24. Hansel TT, Kropshofer H, Singer T, Mitchell JA, George AJ. The safety and side effects of monoclonal antibodies. *Nat Rev Drug Discov.* (2010) 9:325–38. doi: 10.1038/nrd3003
25. Kenanova V, Wu AM. Tailoring antibodies for radionuclide delivery. *Expert Opin Drug Deliv.* (2006) 3:53–70. doi: 10.1517/17425247.3.1.53
26. Orcutt KD, Adams GP, Wu AM, Silva MD, Harwell C, Hoppin J, et al. Molecular Simulation of Receptor Occupancy and Tumor Penetration of an Antibody and Smaller Scaffolds: Application to Molecular Imaging. *Mol Imaging Biol.* (2017) 19:656–64. doi: 10.1007/s11307-016-1041-y
27. Fu R, Carroll L, Yahioglu G, Aboagye EO, Miller PW. Antibody Fragment and Affibody ImmunoPET Imaging Agents: Radiolabelling Strategies and Applications. *ChemMedChem.* (2018) 13:2466–78. doi: 10.1002/cmdc.201800624
28. Weisser NE, Hall JC. Applications of single-chain variable fragment antibodies in therapeutics and diagnostics. *Biotechnol Adv.* (2009) 27:502–20. doi: 10.1016/j.biotechadv.2009.04.004
29. Olafsen T, Wu AM. Antibody vectors for imaging. *Semin Nucl Med.* (2010) 40:167–81. doi: 10.1053/j.semnuclmed.2009.12.005
30. Hu S, Shively L, Raubitschek A, Sherman M, Williams LE, Wong JY, et al. Minibody: A novel engineered anti-carcinoembryonic antigen antibody fragment (single-chain Fv-CH3) which exhibits rapid, high-level targeting of xenografts. *Cancer Res.* (1996) 56:3055–61.
31. Salvador JP, Vilaplana L, Marco MP. Nanobody: outstanding features for diagnostic and therapeutic applications. *Anal Bioanal Chem.* (2019) 411:1703–13. doi: 10.1007/s00216-019-01633-4
32. Divgi CR, Uzzo RG, Gatsonis C, Bartz R, Treutner S, Yu JQ, et al. Positron emission tomography/computed tomography identification of clear cell renal cell carcinoma: results from the REDECT trial. *J Clin Oncol.* (2013) 31:187–94. doi: 10.1200/JCO.2011.41.2445
33. Divgi CR, Pandit-Taskar N, Jungbluth AA, Reuter VE, Gönen M, Ruan S, et al. Preoperative characterisation of clear-cell renal carcinoma using iodine-124-labelled antibody chimeric G250 (124I-cG250) and PET in patients with renal masses: a phase I trial. *Lancet Oncol.* (2007) 8:304–10. doi: 10.1016/S1470-2045(07)70044-X
34. O'Donoghue JA, Smith-Jones PM, Humm JL, Ruan S, Pryma DA, Jungbluth AA, et al. 124I-huA33 antibody uptake is driven by A33 antigen concentration in tissues from colorectal cancer patients imaged by immuno-PET. *J Nucl Med.* (2011) 52:1878–85. doi: 10.2967/jnumed.111.095596
35. Behnam Azad B, Lisok A, Chatterjee S, Poirier JT, Pullambhatla M, Luker GD, et al. Targeted imaging of the atypical chemokine receptor 3 (ACKR3/CXCR7) in human cancer xenografts. *J Nucl Med.* (2016) 57:981–8. doi: 10.2967/jnumed.115.167932
36. Liu S, Li D, Guo J, Canale N, Li X, Liu R, et al. Design, synthesis, and validation of Axl-targeted monoclonal antibody probe for microPET imaging in human lung cancer xenograft. *Mol Pharm.* (2014) 11:3974–9. doi: 10.1021/mp500307t
37. Fung K, Vivier D, Keinänen O, Sarbisheh EK, Price EW. Zeglis BM. (89)Zr-Labeled AR205: A MUC1-Targeting. *ImmunoPET Probe Molecules.* (2020) 25:2315. doi: 10.3390/molecules25102315
38. Sharma SK, Mack KN, Piersigilli A, Pourat J, Edwards KJ, Keinänen O. et al. ImmunoPET of ovarian and pancreatic cancer with AR96, a Novel MUC16-targeted therapeutic antibody. *Clin Cancer Res.* (2022) 28:948–59. doi: 10.1158/1078-0432.CCR-21-1798
39. Nicolazzi C, Caron A, Tellier A, Trombe M, Pinkas J, Payne G, et al. An antibody-drug conjugate targeting MUC1-associated carbohydrate CA6 shows promising antitumor activities. *Mol Cancer Ther.* (2020) 19:1660–9. doi: 10.1158/1535-7163.MCT-19-0826
40. Cepa A, Ráliš J, Král V, Paurová M, Kučka J, Humajová J, et al. In vitro evaluation of the monoclonal antibody (64)Cu-IgG M75 against human carbonic anhydrase IX and its in vivo imaging. *Appl Radiat Isot.* (2018) 133:9–13. doi: 10.1016/j.apradiso.2017.12.013
41. Fujiwara K, Tsuji AB, Sudo H, Sugyo A, Akiba H, Iwanari H, et al. (111)In-labeled anti-cadherin17 antibody D2101 has potential as a noninvasive imaging probe for diagnosing gastric cancer and lymph-node metastasis. *Ann Nucl Med.* (2020) 34:13–23. doi: 10.1007/s12149-019-01408-y
42. Tanaka T. "Leukocyte adhesion molecules," In: Ratcliffe MJH, editor. *Encyclopedia of Immunobiology*. Oxford: Academic Press (2016), p. 505–11.
43. Kang L, Jiang D, Ehlerding EB, Barnhart TE Ni D, Engle JW, et al. Noninvasive trafficking of brentuximab vedotin and PET imaging of CD30 in lung cancer murine models. *Mol Pharm.* (2018) 15:1627–34. doi: 10.1021/acs.molpharmaceut.7b01168
44. Ehlerding EB, England CG, Jiang D, Graves SA, Kang L, Lacognata S, et al. CD38 as a PET imaging target in lung cancer. *Mol Pharm.* (2017) 14:2400–6. doi: 10.1021/acs.molpharmaceut.7b00298
45. Chen C, Zhao S, Karnad A, Freeman JW. The biology and role of CD44 in cancer progression: therapeutic implications. *J Hematol Oncol.* (2018) 11:64. doi: 10.1186/s13045-018-0605-5
46. Spiegelberg D, Nilvebrant J. CD44v6-Targeted imaging of head and neck squamous cell carcinoma: antibody-based approaches. *Contrast Media Mol Imaging.* (2017) 2017:2709547. doi: 10.1155/2017/2709547

47. Zhao H-J, Pan F, Shi Y-C, Luo X, Ren R-R, Peng L-H, et al. Prognostic significance of CD47 in human malignancies: a systematic review and meta-analysis. *Transl Cancer Res.* (2018) 7:609–21. doi: 10.21037/tcr.2018.05.31
48. Wu Y, Wu PY. CD133 as a marker for cancer stem cells: progresses and concerns. *Stem Cells Dev.* (2009) 18:1127–34. doi: 10.1089/scd.2008.0338
49. Sun H, England CG, Hernandez R, Graves SA, Majewski RL, Kamkaew A, et al. ImmunoPET for assessing the differential uptake of a CD146-specific monoclonal antibody in lung cancer. *Eur J Nucl Med Mol Imaging.* (2016) 43:2169–79. doi: 10.1007/s00259-016-3442-1
50. England CG, Jiang D, Hernandez R, Sun H, Valdovinos HF, Ehlerding EB, et al. ImmunoPET imaging of CD146 in murine models of intrapulmonary metastasis of non-small cell lung cancer. *Mol Pharm.* (2017) 14:3239–47. doi: 10.1021/acs.molpharmaceut.7b00216
51. Sugyo A, Tsuji AB, Sudo H, Nagatsu K, Koizumi M, Ukai Y, et al. Evaluation of (89)Zr-labeled human anti-CD147 monoclonal antibody as a positron emission tomography probe in a mouse model of pancreatic cancer. *PLoS One.* (2013) 8:e61230. doi: 10.1371/journal.pone.0061230
52. Kryza T, Khan T, Puttick S, Li C, Sokolowski KA, Tse BW, et al. Effective targeting of intact and proteolysed CDCP1 for imaging and treatment of pancreatic ductal adenocarcinoma. *Theranostics.* (2020) 10:4116–33. doi: 10.7150/thno.43589
53. Su BB, Shi H, Wan J. Role of serum carcinoembryonic antigen in the detection of colorectal cancer before and after surgical resection. *World J Gastroenterol.* (2012) 18:2121–6. doi: 10.3748/wjg.v18.i17.2121
54. Imamura M, Morimoto T, Nomura T, Michishita S, Nishimukai A, Higuchi T, et al. Independent prognostic impact of preoperative serum carcinoembryonic antigen and cancer antigen 15-3 levels for early breast cancer subtypes. *World J Surg Oncol.* (2018) 16:26. doi: 10.1186/s12957-018-1325-6
55. Campos-da-Paz M, Dórea JG, Galdino AS, Lacava ZGM, de Fatima Menezes Almeida Santos M. Carcinoembryonic antigen (CEA) and hepatic metastasis in colorectal cancer: update on biomarker for clinical and biotechnological approaches. *Recent Pat Biotechnol.* (2018) 12:269–79. doi: 10.2174/1872208312666180731104244
56. Ehlerding EB, England CG, Majewski RL, Valdovinos HF, Jiang D, Liu G, et al. ImmunoPET imaging of CTLA-4 expression in mouse models of non-small cell lung cancer. *Mol Pharm.* (2017) 14:1782–9. doi: 10.1021/acs.molpharmaceut.7b00056
57. Liu H, Nie X, Tian Z, Chen D, Chen X, Zeng Q, et al. Single-domain antibodies for radio nuclear imaging and therapy of esophageal squamous cell carcinoma: a narrative review. *J Bio-X Res.* (2020) 3:135–43. doi: 10.1097/JBR.0000000000000074
58. Zhou B, Wang H, Liu R, Wang M, Deng H, Giglio BC, et al. PET Imaging of Dll4 expression in glioblastoma and colorectal cancer xenografts using (64)cu-labeled monoclonal antibody 61B. *Mol Pharm.* (2015) 12:3527–34. doi: 10.1021/acs.molpharmaceut.5b00105
59. Jailkhani N, Ingram JR, Rashidian M, Rickelt S, Tian C, Mak H, et al. Noninvasive imaging of tumor progression, metastasis, and fibrosis using a nanobody targeting the extracellular matrix. *Proc Natl Acad Sci U S A.* (2019) 116:14181–90. doi: 10.1073/pnas.1817442116
60. Hong H, Yang Y, Zhang Y, Engle JW, Barnhart TE, Nickles RJ, et al. Positron emission tomography imaging of CD105 expression during tumor angiogenesis. *Eur J Nucl Med Mol Imaging.* (2011) 38:1335–43. doi: 10.1007/s00259-011-1765-5
61. Trzpis M, McLaughlin PM, de Leij LM, Harmsen MC. Epithelial cell adhesion molecule: more than a carcinoma marker and adhesion molecule. *Am J Pathol.* (2007) 171:386–95. doi: 10.2353/ajpath.2007.070152
62. Fitzgerald AA, Weiner LM. The role of fibroblast activation protein in health and malignancy. *Cancer Metastasis Rev.* (2020) 39:783–803. doi: 10.1007/s10555-020-09909-3
63. Tang W, Huang C, Tang C, Xu J, Wang H. Galectin-3 may serve as a potential marker for diagnosis and prognosis in papillary thyroid carcinoma: a meta-analysis. *Onco Targets Ther.* (2016) 9:455–60. doi: 10.2147/OTT.S94514
64. Krebs S, Carter L, Hirschhorn-Cymerman D, Wolchok J, Merghoub T, Schoder H, et al. Immuno-PET imaging of activation markers on antigen-specific CD4 T cells in a mouse model of melanoma. *J Nucl Med.* (2019) 60:609.
65. Gao W, Ho M. The role of glypican-3 in regulating Wnt in hepatocellular carcinomas. *Cancer Rep.* (2011) 1:14–9.
66. Wang H, Li D, Liu S, Liu R, Yuan H, Krasnoperov V, et al. Small-Animal PET imaging of pancreatic cancer xenografts using a 64cu-labeled monoclonal antibody, MAb159. *J Nucl Med.* (2015) 56:908–13. doi: 10.2967/jnumed.115.155812
67. Aerts HJ, Dubois L, Perk L, Vermaelen P, van Dongen GA, Wouters BG, et al. Disparity between in vivo EGFR expression and 89Zr-labeled cetuximab uptake assessed with PET. *J Nucl Med.* (2009) 50:123–31. doi: 10.2967/jnumed.108.054312
68. Ross JS, Slodkowska EA, Symmans WF, Pusztai L, Ravdin PM, Hortobagyi GN. The HER-2 receptor and breast cancer: ten years of targeted anti-HER-2 therapy and personalized medicine. *Oncologist.* (2009) 14:320–68. doi: 10.1634/theoncologist.2008-0230
69. Yuan Q, Furukawa T, Tashiro T, Okita K, Jin ZH, Aung W, et al. Immuno-PET Imaging of HER3 in a Model in which HER3 signaling plays a critical role. *PLoS One.* (2015) 10:e0143076. doi: 10.1371/journal.pone.0143076
70. Corso S, Giordano S. Cell-autonomous and non-cell-autonomous mechanisms of HGF/MET-driven resistance to targeted therapies: from basic research to a clinical perspective. *Cancer Discov.* (2013) 3:978–92. doi: 10.1158/2159-8290.CD-13-0040
71. Thorek DL, Watson PA, Lee SG, Ku AT, Bournazos S, Braun K, et al. Internalization of secreted antigen-targeted antibodies by the neonatal Fc receptor for precision imaging of the androgen receptor axis. *Sci Transl Med.* (2016) 8:367ra167. doi: 10.1126/scitranslmed.aaf2335
72. Wei W, Jiang D, Lee HJ Li M, Kutyreff CJ, Engle JW, et al. Development and characterization of CD54-targeted immunoPET imaging in solid tumors. *Eur J Nucl Med Mol Imaging.* (2020) 47:2765–75. doi: 10.1007/s00259-020-04784-0
73. Xiao Z, Mayer AT, Nobashi TW, Gambhir SS, ICOS. Is an indicator of T-cell-mediated response to cancer immunotherapy. *Cancer Res.* (2020) 80:3023–32. doi: 10.1158/0008-5472.CAN-19-3265
74. Heskamp S, van Laarhoven HW, Molkenboer-Kuenen JD, Franssen GM, Versleijen-Jonkers YM, Oyen WJ, et al. ImmunoSPECT and immunoPET of IGF-1R expression with the radiolabeled antibody R1507 in a triple-negative breast cancer model. *J Nucl Med.* (2010) 51:1565–72. doi: 10.2967/jnumed.110.075648
75. White JB, Hu LY, Boucher DL, Sutcliffe JL. ImmunoPET Imaging of α(v)β(6) Expression using an engineered anti-α(v)β(6) cys-diabody site-specifically radiolabeled with Cu-64: considerations for optimal imaging with antibody fragments. *Mol Imaging Biol.* (2018) 20:103–13. doi: 10.1007/s11307-017-1097-3
76. Kim HR, Song IH, Lee TS, Hong HJ, An GI, Kim KI, et al. Immuno-PET and activatable near-infrared fluorescence dual-modality imaging of L1-CAM expression in cholangiocarcinoma model. *J Nucl Med.* (2016) 57:1213.
77. Gong X, Azhdarinia A, Ghosh SC, Xiong W, An Z, Liu Q, et al. LGR5-Targeted antibody-drug conjugate eradicates gastrointestinal tumors and prevents recurrence. *Mol Cancer Ther.* (2016) 15:1580–90. doi: 10.1158/1535-7163.MCT-16-0114
78. Mandleywala K, Shmuel S, Pereira PMR, Lewis JS. Antibody-targeted imaging of gastric cancer. *Molecules.* (2020) 25:20. doi: 10.3390/molecules25204621
79. Tang Z, Qian M, Ho M. The role of mesothelin in tumor progression and targeted therapy. *Anticancer Agents Med Chem.* (2013) 13:276–80. doi: 10.2174/1871520611313020014
80. Morcillo M, García de. Lucas Á, Oteo M, Romero E, Magro N, Ibáñez M, et al. MT1-MMP as a PET imaging biomarker for pancreas cancer management contrast media. *Mol Imaging.* (2018) 2018:8382148. doi: 10.1155/2018/8382148
81. Schütz F, Stefanovic S, Mayer L, von Au A, Domschke C, Sohn C. PD-1/PD-L1 Pathway in Breast Cancer. *Oncol Res Treat.* (2017) 40:294–7. doi: 10.1159/000464353
82. Cai H, Shi Q, Tang Y, Chen L, Chen Y, Tao Z, et al. Positron emission tomography imaging of platelet-derived growth factor receptor β in colorectal tumor xenograft using zirconium-89 labeled dimeric affibody molecule. *Mol Pharm.* (2019) 16:1950–7. doi: 10.1021/acs.molpharmaceut.8b01317
83. Rousseau C, Ruellan AL, Bernardeau K, Kraeber-Bodere F, Gouard S, Loussouarn D, et al. Syndecan-1 antigen, a promising new target for triple-negative breast cancer immuno-PET and radioimmunotherapy. A

preclinical study on MDA-MB-468 xenograft tumors. *EJNMMI Res.* (2011) 1:20. doi: 10.1186/2191-219X-1-20
84. Heidari P, Esfahani SA, Turker NS, Wong G, Wang TC, Rustgi AK, et al. Imaging of secreted extracellular periostin, an important marker of invasion in the tumor microenvironment in esophageal cancer. *J Nucl Med.* (2015) 56:1246–51. doi: 10.2967/jnumed.115.156216
85. Zhu H, Liu TL, Liu CH, Wang J, Zhang H, Dong B, et al. Evaluation of a novel monoclonal antibody mAb109 by immuno-PET/fluorescent imaging for noninvasive lung adenocarcinoma diagnosis. *Acta Pharmacol Sin.* (2020) 41:101–9. doi: 10.1038/s41401-019-0294-9
86. Oesterling JE. Prostate-specific antigen and diagnosing early malignancies of the prostate. *J Cell Biochem Suppl.* (1992) 16h:31–43. doi: 10.1002/jcb.240501209
87. Knowles SM, Tavaré R, Zettlitz KA, Rochefort MM, Salazar FB, Jiang ZK, et al. Applications of immunoPET: using 124I-anti-PSCA A11 minibody for imaging disease progression and response to therapy in mouse xenograft models of prostate cancer. *Clin Cancer Res.* (2014) 20:6367–78. doi: 10.1158/1078-0432.CCR-14-1452
88. Bander NH, Nanus DM, Milowsky MI, Kostakoglu L, Vallabahajosula S, Goldsmith SJ. Targeted systemic therapy of prostate cancer with a monoclonal antibody to prostate-specific membrane antigen. *Semin Oncol.* (2003) 30:667–76. doi: 10.1016/S0093-7754(03)00358-0
89. Yamagishi S, Matsui T, Fukami K. Role of receptor for advanced glycation end products (RAGE) and its ligands in cancer risk. *Rejuvenation Res.* (2015) 18:48–56. doi: 10.1089/rej.2014.1625
90. Dewulf J, Vangestel C, Verhoeven Y, De Waele J, Zwaenepoel K, van Dam PA, et al. Immuno-PET molecular imaging of RANKL in cancer. *Cancers (Basel).* (2021) 13:2166. doi: 10.3390/cancers13092166
91. Cho J, Kim KM, Kim HC, Lee WY, Kang WK, Park YS, et al. The prognostic role of tumor associated glycoprotein 72 (TAG-72) in stage II and III colorectal adenocarcinoma. *Pathol Res Pract.* (2019) 215:171–6. doi: 10.1016/j.prp.2018.10.024
92. Kim HY Li R, Ng TSC, Courties G, Rodell CB, Prytyskach M, et al. Quantitative Imaging of Tumor-Associated Macrophages and Their Response to Therapy Using (64)Cu-Labeled Macrin. *ACS Nano.* (2018) 12:12015–29. doi: 10.1021/acsnano.8b04338
93. Hernandez R, England CG, Yang Y, Valdovinos HF, Liu B, Wong HC, et al. ImmunoPET imaging of tissue factor expression in pancreatic cancer with (89)Zr-Df-ALT-836. *J Control Release.* (2017) 264:160–8. doi: 10.1016/j.jconrel.2017.08.029
94. Sugyo A, Tsuji AB, Sudo H, Nagatsu K, Koizumi M, Ukai Y, et al. Preclinical evaluation of 8?Zr-labeled human antitransferrin receptor monoclonal antibody as a PET probe using a pancreatic cancer mouse model. *Nucl Med Commun.* (2015) 36:286–94. doi: 10.1097/MNM.0000000000000245
95. den Hollander MW, Bensch F, Glaudemans AW, Oude Munnink TH, Enting RH, den Dunnen WF, et al. TGF-β Antibody Uptake in Recurrent High-Grade Glioma Imaged with 89Zr-Fresolimumab PET. *J Nucl Med.* (2015) 56:1310–4. doi: 10.2967/jnumed.115.154401
96. Gooden MJ, de Bock GH, Leffers N, Daemen T, Nijman HW. The prognostic influence of tumour-infiltrating lymphocytes in cancer: a systematic review with meta-analysis. *Br J Cancer.* (2011) 105:93–103. doi: 10.1038/bjc.2011.189
97. Wei W, Jiang D, Lee HJ, Engle JW, Akiba H, Liu J, et al. ImmunoPET imaging of TIM-3 in murine melanoma models. *Adv Ther (Weinh).* (2020) 3:2000018. doi: 10.1002/adtp.202000018
98. White JM, Kuda-Wedagedara AN, Wicker MN, Spratt DE, Schopperle WM, Heath E, et al. Detecting TRA-1-60 in Cancer via a Novel Zr-89 Labeled ImmunoPET Imaging Agent. *Mol Pharm.* (2020) 17:1139–47. doi: 10.1021/acs.molpharmaceut.9b01181
99. Shvartsur A, Bonavida B. Trop2 and its overexpression in cancers: regulation and clinical/therapeutic implications. *Genes Cancer.* (2015) 6:84–105. doi: 10.18632/genesandcancer.40
100. do Espírito Santo GF, Galera BB, Duarte EC, Chen ES, Azis L, Damazo AS, et al. Prognostic significance of vascular endothelial growth factor polymorphisms in colorectal cancer patients. *World J Gastrointest Oncol.* (2017) 9:78–86. doi: 10.4251/wjgo.v9.i2.78
101. Kramer-Marek G, Oyen WJ. Targeting the human epidermal growth factor receptors with immuno-PET: imaging biomarkers from bench to bedside. *J Nucl Med.* (2016) 57:996–1001. doi: 10.2967/jnumed.115.169540
102. Dijkers EC, Oude Munnink TH, Kosterink JG, Brouwers AH, Jager PL, de Jong JR, et al. Biodistribution of 89Zr-trastuzumab and PET imaging of HER2-positive lesions in patients with metastatic breast cancer. *Clin Pharmacol Ther.* (2010) 87:586–92. doi: 10.1038/clpt.2010.12
103. Lockhart AC, Liu Y, Dehdashti F, Laforest R, Picus J, Frye J, et al. Phase 1 evaluation of [(64)Cu]DOTA-patritumab to assess dosimetry, apparent receptor occupancy, and safety in subjects with advanced solid tumors. *Mol Imaging Biol.* (2016) 18:446–53. doi: 10.1007/s11307-015-0912-y
104. Menke-van der Houven van Oordt CW, McGeoch A, Bergstrom M, McSherry I, Smith DA, Cleveland M, et al. Immuno-PET Imaging to Assess Target Engagement: Experience from (89)Zr-Anti-HER3 mAb (GSK2849330) in Patients with Solid Tumors. *J Nucl Med.* (2019) 60:902–9. doi: 10.2967/jnumed.118.214726
105. Warnders FJ, Terwisscha van Scheltinga AGT, Knuehl C, van Roy M, de Vries EFJ, Kosterink JGW, et al. Human Epidermal Growth Factor Receptor 3-Specific Tumor Uptake and Biodistribution of (89)Zr-MSB0010853 Visualized by Real-Time and Noninvasive *PET Imaging. J Nucl Med.* (2017) 58:1210–5. doi: 10.2967/jnumed.116.181586
106. Rosestedt M, Andersson KG, Mitran B, Tolmachev V, Löfblom J, Orlova A, et al. Affibody-mediated PET imaging of HER3 expression in malignant tumours. *Sci Rep.* (2015) 5:15226. doi: 10.1038/srep15226
107. van Asselt SJ, Oosting SF, Brouwers AH, Bongaerts AH, de Jong JR. Lub-de Hooge MN, et al. Everolimus reduces (89)Zr-bevacizumab tumor uptake in patients with neuroendocrine tumors. *J Nucl Med.* (2014) 55:1087–92. doi: 10.2967/jnumed.113.129056
108. Jauw YW. Menke-van der Houven van Oordt CW, Hoekstra OS, Hendrikse NH, Vugts DJ, Zijlstra JM, et al. Immuno-positron emission tomography with zirconium-89-labeled monoclonal antibodies in oncology: what can we learn from initial clinical trials? *Front Pharmacol.* (2016) 7:131. doi: 10.3389/fphar.2016.00131
109. Mortimer JE, Bading JR, Colcher DM, Conti PS, Frankel PH, Carroll MI, et al. Functional imaging of human epidermal growth factor receptor 2-positive metastatic breast cancer using (64)Cu-DOTA-trastuzumab PET. *J Nucl Med.* (2014) 55:23–9. doi: 10.2967/jnumed.113.122630
110. Pool M, Kol A. Lub-de Hooge MN, Gerdes CA, de Jong S, de Vries EG, et al. Extracellular domain shedding influences specific tumor uptake and organ distribution of the EGFR PET tracer 89Zr-imgatuzumab. *Oncotarget.* (2016) 7:68111–21. doi: 10.18632/oncotarget.11827
111. van Loon J, Even AJG, Aerts H, Öllers M, Hoebers F, van Elmpt W, et al. PET imaging of zirconium-89 labelled cetuximab: A phase I trial in patients with head and neck and lung cancer. *Radiother Oncol.* (2017) 122:267–73. doi: 10.1016/j.radonc.2016.11.020
112. Keyaerts M, Xavier C, Heemskerk J, Devoogdt N, Everaert H, Ackaert C, et al. Phase I Study of 68Ga-HER2-Nanobody for PET/CT Assessment of HER2 Expression in Breast Carcinoma. *J Nucl Med.* (2016) 57:27–33. doi: 10.2967/jnumed.115.162024
113. Beylergil V, Morris PG, Smith-Jones PM, Modi S, Solit D, Hudis CA, et al. Pilot study of 68Ga-DOTA-F(ab')2-trastuzumab in patients with breast cancer. *Nucl Med Commun.* (2013) 34:1157–65. doi: 10.1097/MNM.0b013e328365d99b
114. Sandström M, Lindskog K, Velikyan I, Wennborg A, Feldwisch J, Sandberg D, et al. Biodistribution and radiation dosimetry of the anti-her2 affibody molecule 68Ga-ABY-025 in breast cancer patients. *J Nucl Med.* (2016) 57:867–71. doi: 10.2967/jnumed.115.169342
115. Velikyan I, Schweighöfer P, Feldwisch J, Seemann J, Frejd FY, Lindman H, et al. Diagnostic HER2-binding radiopharmaceutical, [(68)Ga]Ga-ABY-025, for routine clinical use in breast cancer patients. *Am J Nucl Med Mol Imaging.* (2019) 9:12–23.
116. Niu G, Li Z, Xie J, Le QT, Chen X, PET. of EGFR antibody distribution in head and neck squamous cell carcinoma models. *J Nucl Med.* (2009) 50:1116–23. doi: 10.2967/jnumed.109.061820
117. Esfahani K, Roudaia L, Buhlaiga N, Del Rincon SV, Papneja N, Miller WH. Jr. A review of cancer immunotherapy: from the past, to the present, to the future. *Curr Oncol.* (2020) 27:S87–s97. doi: 10.3747/co.27.5223

118. Niemeijer AN, Leung D, Huisman MC, Bahce I, Hoekstra OS, van Dongen G, et al. Whole body PD-1 and PD-L1 positron emission tomography in patients with non-small-cell lung cancer. *Nat Commun.* (2018) 9:4664. doi: 10.1038/s41467-018-07131-y
119. van der Veen EL, Giesen D. Pot-de Jong L, Jorritsma-Smit A, De Vries EGE, Lub-de Hooge MN. *(*89)Zr-pembrolizumab biodistribution is influenced by PD-1-mediated uptake in lymphoid organs. *J Immunother Cancer.* (2020) 8:e000938. doi: 10.1136/jitc-2020-000938
120. Zhao J, Wen X, Li T, Shi S, Xiong C, Wang YA, et al. Concurrent injection of unlabeled antibodies allows positron emission tomography imaging of programmed cell death ligand 1 expression in an orthotopic pancreatic tumor model. *ACS Omega.* (2020) 5:8474–82. doi: 10.1021/acsomega.9b03731
121. Azimi F, Scolyer RA, Rumcheva P, Moncrieff M, Murali R, McCarthy SW, et al. Tumor-infiltrating lymphocyte grade is an independent predictor of sentinel lymph node status and survival in patients with cutaneous melanoma. *J Clin Oncol.* (2012) 30:2678–83. doi: 10.1200/JCO.2011.37.8539
122. Kristensen LK, Fröhlich C, Christensen C, Melander MC, Poulsen TT, Galler GR, et al. CD4(+) and CD8a(+) PET imaging predicts response to novel PD-1 checkpoint inhibitor: studies of Sym021 in syngeneic mouse cancer models. *Theranostics.* (2019) 9:8221–38. doi: 10.7150/thno.37513
123. Tavaré R, Escuin-Ordinas H, Mok S, McCracken MN, Zettlitz KA, Salazar FB, et al. An Effective Immuno-PET Imaging Method to Monitor CD8-Dependent Responses to Immunotherapy. *Cancer Res.* (2016) 76:73–82. doi: 10.1158/0008-5472.CAN-15-1707
124. Rashidian M, LaFleur MW, Verschoor VL, Dongre A, Zhang Y, Nguyen TH, et al. Immuno-PET identifies the myeloid compartment as a key contributor to the outcome of the antitumor response under PD-1 blockade. *Proc Natl Acad Sci U S A.* (2019) 116:16971–80. doi: 10.1073/pnas.1905005116
125. Kristensen LK, Christensen C, Alfsen MZ, Cold S, Nielsen CH, Kjaer A. Monitoring CD8a(+) T cell responses to radiotherapy and CTLA-4 blockade using [(64)Cu]NOTA-CD8a PET imaging. *Mol Imaging Biol.* (2020) 22:1021–30. doi: 10.1007/s11307-020-01481-0
126. Seo JW, Tavaré R, Mahakian LM, Silvestrini MT, Tam S, Ingham ES, et al. CD8(+) T-Cell density imaging with (64)Cu-Labeled Cys-diabody informs immunotherapy protocols. *Clin Cancer Res.* (2018) 24:4976–87. doi: 10.1158/1078-0432.CCR-18-0261
127. Wang J, Xu B. Targeted therapeutic options and future perspectives for HER2-positive breast cancer. *Signal Transduct Target Ther.* (2019) 4:34. doi: 10.1038/s41392-019-0069-2
128. Ulaner GA, Riedl CC, Dickler MN, Jhaveri K, Pandit-Taskar N, Weber W. Molecular Imaging of Biomarkers in Breast Cancer. *J Nucl Med.* (2016) 57:53s–9s. doi: 10.2967/jnumed.115.157909
129. Massicano AVF, Marquez-Nostra BV, Lapi SE. Targeting HER2 in nuclear medicine for imaging and therapy. *Mol Imaging.* (2018) 17:1536012117745386. doi: 10.1177/1536012117745386
130. Ulaner GA, Hyman DM, Lyashchenko SK, Lewis JS, Carrasquillo JA. 89Zr-Trastuzumab PET/CT for detection of human epidermal growth factor receptor 2-positive metastases in patients with human epidermal growth factor receptor 2-negative primary breast cancer. *Clin Nucl Med.* (2017) 42:912–7. doi: 10.1097/RLU.0000000000001820
131. Ulaner GA, Lyashchenko SK, Riedl C, Ruan S, Zanzonico PB, Lake D, et al. First-in-human human epidermal growth factor receptor 2-targeted imaging using (89)Zr-Pertuzumab PET/CT: dosimetry and clinical application in patients with breast cancer. *J Nucl Med.* (2018) 59:900–6. doi: 10.2967/jnumed.117.202010
132. Marquez BV, Ikotun OF, Zheleznyak A, Wright B, Hari-Raj A, Pierce RA, et al. Evaluation of (89)Zr-pertuzumab in Breast cancer xenografts. *Mol Pharm.* (2014) 11:3988–95. doi: 10.1021/mp500323d
133. Wimana Z, Gebhart G, Guiot T, Vanderlinden B, Morandini R, Doumont G, et al. Mucolytic agents can enhance her2 receptor accessibility for [(89)Zr]trastuzumab, improving HER2 imaging in a mucin-overexpressing breast cancer xenograft mouse Model. *Mol Imaging Biol.* (2015) 17:697–703. doi: 10.1007/s11307-015-0840-x
134. Laforest R, Lapi SE, Oyama R, Bose R, Tabchy A, Marquez-Nostra BV, et al. [(89)Zr]Trastuzumab: evaluation of radiation dosimetry, safety, and optimal imaging parameters in women with HER2-positive breast cancer. *Mol Imaging Biol.* (2016) 18:952–9. doi: 10.1007/s11307-016-0951-z
135. Tamura K, Kurihara H, Yonemori K, Tsuda H, Suzuki J, Kono Y, et al. 64Cu-DOTA-trastuzumab PET imaging in patients with HER2-positive breast cancer. *J Nucl Med.* (2013) 54:1869–75. doi: 10.2967/jnumed.112.118612
136. Bensch F, Brouwers AH. Lub-de Hooge MN, de Jong JR, van der Vegt B, Sleijfer S, et al. *(*89)Zr-trastuzumab PET supports clinical decision making in breast cancer patients, when HER2 status cannot be determined by standard work up. *Eur J Nucl Med Mol Imaging.* (2018) 45:2300–6. doi: 10.1007/s00259-018-4099-8
137. Gaykema SB, Schröder CP, Vitfell-Rasmussen J, Chua S, Oude Munnink TH, Brouwers AH, et al. 89Zr-trastuzumab and 89Zr-bevacizumab PET to evaluate the effect of the HSP90 inhibitor NVP-AUY922 in metastatic breast cancer patients. *Clin Cancer Res.* (2014) 20:3945–54. doi: 10.1158/1078-0432.CCR-14-0491
138. Lam K, Chan C, Reilly RM. Development and preclinical studies of (64)Cu-NOTA-pertuzumab F(ab')(2) for imaging changes in tumor HER2 expression associated with response to trastuzumab by PET/CT. *MAbs.* (2017) 9:154–64. doi: 10.1080/19420862.2016.1255389
139. Mendler CT, Gehring T, Wester HJ, Schwaiger M, Skerra A. 8?Zr-Labeled Versus ^{124}I-Labeled αHER2 fab with optimized plasma half-life for high-contrast tumor imaging in vivo. *J Nucl Med.* (2015) 56:1112–8. doi: 10.2967/jnumed.114.149690
140. Kwon LY, Scollard DA, Reilly RM. (64)Cu-Labeled Trastuzumab Fab-PEG(24)-EGF Radioimmunoconjugates Bispecific for HER2 and EGFR: Pharmacokinetics, Biodistribution, and Tumor Imaging by PET in comparison to monospecific agents. *Mol Pharm.* (2017) 14:492–501. doi: 10.1021/acs.molpharmaceut.6b00963
141. Glaser M, Iveson P, Hoppmann S, Indrevoll B, Wilson A, Arukwe J, et al. Three methods for 18F labeling of the HER2-binding affibody molecule Z(HER2:2891) including preclinical assessment. *J Nucl Med.* (2013) 54:1981–8. doi: 10.2967/jnumed.113.122465
142. Sörensen J, Velikyan I, Sandberg D, Wennborg A, Feldwisch J, Tolmachev V, et al. Measuring HER2-receptor expression in metastatic breast cancer using [68Ga] ABY-025 Affibody PET/CT. *Theranostics.* (2016) 6:262. doi: 10.7150/thno.13502
143. Emens LA, Braiteh FS, Cassier P, Delord J-P, Eder JP, Fasso M, et al. Inhibition of PD-L1 by MPDL3280A leads to clinical activity in patients with metastatic triple-negative breast cancer (TNBC). *AACR.* (2015). doi: 10.1158/1538-7445.AM2015-2859
144. Bensch F, van der Veen EL. Lub-de Hooge MN, Jorritsma-Smit A, Boellaard R, Kok IC, et al. (89)Zr-atezolizumab imaging as a non-invasive approach to assess clinical response to PD-L1 blockade in cancer. *Nat Med.* (2018) 24:1852–8. doi: 10.1038/s41591-018-0255-8
145. Li M, Ehlerding EB, Jiang D, Barnhart TE, Chen W, Cao T, et al. In vivo characterization of PD-L1 expression in breast cancer by immuno-PET with (89)Zr-labeled avelumab. *Am J Transl Res.* (2020) 12:1862–72.
146. Jagoda EM, Vasalatiy O, Basuli F, Opina ACL, Williams MR, Wong K, et al. Immuno-PET imaging of the programmed cell death-1 Ligand (PD-L1) using a zirconium-89 labeled therapeutic antibody, avelumab. *Mol Imaging.* (2019) 18:1536012119829986. doi: 10.1177/1536012119829986
147. Bodet-Milin C, Bailly C, Touchefeu Y, Frampas E, Bourgeois M, Rauscher A, et al. Clinical results in medullary thyroid carcinoma suggest high potential of pretargeted immuno-PET for tumor imaging and theranostic approaches. *Front Med (Lausanne).* (2019) 6:124. doi: 10.3389/fmed.2019.00124
148. Pichon B, Rousseau C, Blanc-Lapierre A, Delpon G, Ferrer L, Libois V, et al. Targeting stereotactic body radiotherapy on metabolic pet- and immuno-pet-positive vertebral metastases. *Biomedicines.* (2020) 8:12. doi: 10.3390/biomedicines8120548
149. Rousseau C, Goldenberg DM, Colombie M, Sebille JC, Meingan P, Ferrer L, et al. Initial clinical results of a novel immuno-PET Theranostic probe in human epidermal growth factor receptor 2-negative breast cancer. *J Nucl Med.* (2020) 61:1205–11. doi: 10.2967/jnumed.119.236000
150. Nagengast WB, de Vries EG, Hospers GA, Mulder NH, de Jong JR, Hollema H, et al. In vivo VEGF imaging with radiolabeled bevacizumab in a human ovarian tumor xenograft. *J Nucl Med.* (2007) 48:1313–9. doi: 10.2967/jnumed.107.041301
151. Gaykema SB, Brouwers AH. Lub-de Hooge MN, Pleijhuis RG, Timmer-Bosscha H, Pot L, et al. 89Zr-bevacizumab PET imaging in primary breast cancer. *J Nucl Med.* (2013) 54:1014–8. doi: 10.2967/jnumed.112.117218

152. Hong H, Severin GW, Yang Y, Engle JW, Zhang Y, Barnhart TE, et al. Positron emission tomography imaging of CD105 expression with 89Zr-Df-TRC105. *Eur J Nucl Med Mol Imaging.* (2012) 39:138–48. doi: 10.1007/s00259-011-1930-x
153. Hong H, Zhang Y, Severin GW, Yang Y, Engle JW, Niu G, et al. Multimodality imaging of breast cancer experimental lung metastasis with bioluminescence and a monoclonal antibody dual-labeled with 89Zr and IRDye 800CW. *Mol Pharm.* (2012) 9:2339–49. doi: 10.1021/mp300277f
154. Zhang Y, Hong H, Orbay H, Valdovinos HF, Nayak TR, Theuer CP, et al. PET imaging of CD105/endoglin expression with a 61/64Cu-labeled Fab antibody fragment. *Eur J Nucl Med Mol Imaging.* (2013) 40:759–67. doi: 10.1007/s00259-012-2334-2
155. Hong H, Zhang Y, Orbay H, Valdovinos HF, Nayak TR, Bean J, et al. Positron emission tomography imaging of tumor angiogenesis with a (61/64)Cu-labeled F(ab')(2) antibody fragment. *Mol Pharm.* (2013) 10:709–16. doi: 10.1007/978-94-007-4945-0
156. Manafi-Farid R, Karamzade-Ziarati N, Vali R, Mottaghy FM, Beheshti M. 2-[(18)F]FDG PET/CT radiomics in lung cancer: An overview of the technical aspect and its emerging role in management of the disease. *Methods.* (2021) 188:84–97. doi: 10.1016/j.ymeth.2020.05.023
157. National Comprehensive Cancer Network (NCCN). *NCCN Clinical Practice Guidelines in Oncology. Non-Small Cell Lung Cancer. Version 1.2022.* (2022). Available online at: https://www.nccn.org/professionals/physician_gls/pdf/nscl.pdf.
158. Nayak TK, Garmestani K, Milenic DE, Baidoo KE, Brechbiel MW. HER1-targeted 86Y-panitumumab possesses superior targeting characteristics than 86Y-cetuximab for PET imaging of human malignant mesothelioma tumors xenografts. *PLoS One.* (2011) 6:e18198. doi: 10.1371/journal.pone.0018198
159. Chang AJ, De Silva RA, Lapi SE. Development and characterization of 89Zr-labeled panitumumab for immuno-positron emission tomographic imaging of the epidermal growth factor receptor. *Mol Imaging.* (2013) 12:17–27.
160. Nayak TK, Garmestani K, Milenic DE, Brechbiel MW, PET. and MRI of metastatic peritoneal and pulmonary colorectal cancer in mice with human epidermal growth factor receptor 1-targeted 89Zr-labeled panitumumab. *J Nucl Med.* (2012) 53:113–20. doi: 10.2967/jnumed.111.094169
161. Paudyal B, Paudyal P, Oriuchi N, Hanaoka H, Tominaga H, Endo K. Positron emission tomography imaging and biodistribution of vascular endothelial growth factor with 64Cu-labeled bevacizumab in colorectal cancer xenografts. *Cancer Sci.* (2011) 102:117–21. doi: 10.1111/j.1349-7006.2010.01763.x
162. Nayak TK, Garmestani K, Baidoo KE, Milenic DE, Brechbiel MW, PET. imaging of tumor angiogenesis in mice with VEGF-A-targeted (86)Y-CHX-A″-DTPA-bevacizumab. *Int J Cancer.* (2011) 128:920–6. doi: 10.1002/ijc.25409
163. Yamaguchi A, Achmad A, Hanaoka H, Heryanto YD, Bhattarai A. Ratianto, et al. Immuno-PET imaging for non-invasive assessment of cetuximab accumulation in non-small cell lung cancer. *BMC Cancer.* (2019) 19:1000. doi: 10.1186/s12885-019-6238-4
164. Luo H, England CG, Graves SA, Sun H, Liu G, Nickles RJ, et al. PET Imaging of VEGFR-2 expression in lung cancer with 64Cu-labeled ramucirumab. *J Nucl Med.* (2016) 57:285–90. doi: 10.2967/jnumed.115.166462
165. Xu X, Liu T, Liu F, Guo X, Xia L, Xie Q, et al. Synthesis and evaluation of (64)Cu-radiolabeled NOTA-cetuximab ((64)Cu-NOTA-C225) for immuno-PET imaging of EGFR expression. *Chin J Cancer Res.* (2019) 31:400–9. doi: 10.21147/j.issn.1000-9604.2019.02.14
166. Bahce I, Huisman MC, Verwer EE, Ooijevaar R, Boutkourt F, Vugts DJ, et al. Pilot study of (89)Zr-bevacizumab positron emission tomography in patients with advanced non-small cell lung cancer. *EJNMMI Res.* (2014) 4:35. doi: 10.1186/s13550-014-0035-5
167. Hsu ML, Naidoo J. Principles of Immunotherapy in Non-Small Cell Lung Cancer. *Thorac Surg Clin.* (2020) 30:187–98. doi: 10.1016/j.thorsurg.2020.01.009
168. National Comprehensive Cancer Network (NCCN). *NCCN Clinical Practice Guidelines in Oncology. Gastric Cancer. Version 2.2022.* (2022). Available online at: https://www.nccn.org/professionals/physician_gls/pdf/gastric.pdf.
169. Liberini V, Laudicella R, Capozza M, Huellner MW, Burger IA, Baldari S, et al. The future of cancer diagnosis, treatment and surveillance: a systemic review on immunotherapy and immuno-pet radiotracers. *Molecules.* (2021) 26:8. doi: 10.3390/molecules26082201
170. Christensen C, Kristensen LK, Alfsen MZ, Nielsen CH, Kjaer A. Quantitative PET imaging of PD-L1 expression in xenograft and syngeneic tumour models using a site-specifically labelled PD-L1 antibody. *Eur J Nucl Med Mol Imaging.* (2020) 47:1302–13. doi: 10.1007/s00259-019-04646-4
171. Jiang J, Zhang M, Li G, Liu T, Wan Y, Liu Z, et al. Evaluation of (64)Cu radiolabeled anti-hPD-L1 Nb6 for positron emission tomography imaging in lung cancer tumor mice model. *Bioorg Med Chem Lett.* (2020) 30:126915. doi: 10.1016/j.bmcl.2019.126915
172. England CG, Jiang D, Ehlerding EB, Rekoske BT, Ellison PA, Hernandez R, et al. (89)Zr-labeled nivolumab for imaging of T-cell infiltration in a humanized murine model of lung cancer. *Eur J Nucl Med Mol Imaging.* (2018) 45:110–20. doi: 10.1007/s00259-017-3803-4
173. Niemeijer AN, Oprea-Lager DE, Huisman MC, Hoekstra OS, Boellaard R. de Wit-van der Veen BJ, et al. Study of (89)Zr-pembrolizumab PET/CT in patients with advanced-stage non-small cell lung cancer. *J Nucl Med.* (2022) 63:362–7. doi: 10.2967/jnumed.121.261926
174. Pandit-Taskar N, Postow MA, Hellmann MD, Harding JJ, Barker CA, O'Donoghue JA, et al. First-in-Humans Imaging with (89)Zr-Df-IAB22M2C Anti-CD8 Minibody in Patients with Solid Malignancies: Preliminary Pharmacokinetics, Biodistribution, and Lesion Targeting. *J Nucl Med.* (2020) 61:512–9. doi: 10.2967/jnumed.119.229781
175. Kang L, Jiang D, Ehlerding E, Ni D, Yu B, Barnhart T, et al. In vivo visualization of brentuximab vedotin and immunoPET of CD30 in lung cancer murine models. *J Nucl Med.* (2018) 59:171.
176. Li K, Tavaré R, Zettlitz KA, Mumenthaler SM, Mallick P, Zhou Y, et al. Anti-MET immunoPET for non-small cell lung cancer using novel fully human antibody fragments. *Mol Cancer Ther.* (2014) 13:2607–17. doi: 10.1158/1535-7163.MCT-14-0363
177. van Scheltinga AGT. Lub-de Hooge MN, Hinner MJ, Verheijen RB, Allersdorfer A, Hülsmeyer M, et al. In vivo visualization of MET tumor expression and anticalin biodistribution with the MET-specific anticalin 89Zr-PRS-110 PET tracer. *J Nucl Med.* (2014) 55:665–71. doi: 10.2967/jnumed.113.124941
178. Kristiansen G, Yu Y, Schlüns K, Sers C, Dietel M, Petersen I. Expression of the cell adhesion molecule CD146/MCAM in non-small cell lung cancer. analytical cellular pathology: the journal of the european society for analytical cellular. *Pathology.* (2003) 25:77–81. doi: 10.1155/2003/574829
179. Olajuyin AM, Olajuyin AK, Wang Z, Zhao X, Zhang X. CD146 T cells in lung cancer: its function, detection, and clinical implications as a biomarker and therapeutic target. *Cancer Cell Int.* (2019) 19:247. doi: 10.1186/s12935-019-0969-9
180. Paudyal P, Paudyal B, Hanaoka H, Oriuchi N, Iida Y, Yoshioka H, et al. Imaging and biodistribution of Her2/neu expression in non-small cell lung cancer xenografts with Cu-labeled trastuzumab PET. *Cancer Sci.* (2010) 101:1045–50. doi: 10.1111/j.1349-7006.2010.01480.x
181. Peeters M, Karthaus M, Rivera F, Terwey JH, Douillard JY. Panitumumab in metastatic colorectal cancer: the importance of tumour RAS status. *Drugs.* (2015) 75:731–48. doi: 10.1007/s40265-015-0386-x
182. Martin B, Märkl B. Immunologic biomarkers and biomarkers for immunotherapies in gastrointestinal cancer. *Visc Med.* (2019) 35:3–10. doi: 10.1159/000496565
183. Van Helden E, Elias S, Gerritse S, van Es S, Boon E, Huisman M, et al. [89Zr] Zr-cetuximab PET/CT as biomarker for cetuximab monotherapy in patients with RAS wild-type advanced colorectal cancer. *Eur J Nucl Med Mol Imaging.* (2020) 47:849–59. doi: 10.1007/s00259-019-04555-6
184. Menke-van der Houven van Oordt CW, Gootjes EC, Huisman MC, Vugts DJ, Roth C, Luik AM, et al. 89Zr-cetuximab PET imaging in patients with advanced colorectal cancer. *Oncotarget.* (2015) 6:30384–93. doi: 10.18632/oncotarget.4672
185. Wei L, Shi J, Afari G, Bhattacharyya S. Preparation of clinical-grade (89) Zr-panitumumab as a positron emission tomography biomarker for evaluating epidermal growth factor receptor-targeted therapy. *J Labelled Comp Radiopharm.* (2014) 57:25–35. doi: 10.1002/jlcr.3134

186. Shi X, Gao K, Huang H, Gao R. Pretargeted Immuno-PET based on bioorthogonal chemistry for imaging EGFR positive colorectal cancer. *Bioconjug Chem.* (2018) 29:250–4. doi: 10.1021/acs.bioconjchem.8b00023
187. Cai W, Olafsen T, Zhang X, Cao Q, Gambhir SS, Williams LE. et al. PET imaging of colorectal cancer in xenograft-bearing mice by use of an 18F-labeled T8466 anti-carcinoembryonic antigen diabody. *J Nucl Med.* (2007) 48:304–10.
188. Sundaresan G, Yazaki PJ, Shively JE, Finn RD, Larson SM, Raubitschek AA, et al. 124I-labeled engineered anti-CEA minibodies and diabodies allow high-contrast, antigen-specific small-animal PET imaging of xenografts in athymic mice. *J Nucl Med.* (2003) 44:1962–9.
189. Bading JR, Hörling M, Williams LE, Colcher D, Raubitschek A, Strand SE. Quantitative serial imaging of an 124I anti-CEA monoclonal antibody in tumor-bearing mice. *Cancer Biother Radiopharm.* (2008) 23:399–409. doi: 10.1089/cbr.2007.0457
190. McBride WJ, Zanzonico P, Sharkey RM, Norén C, Karacay H, Rossi EA, et al. Bispecific antibody pretargeting PET (immunoPET) with an 124I-labeled hapten-peptide. *J Nucl Med.* (2006) 47:1678−88.
191. Hall H, Velikyan I, Blom E, Ulin J, Monazzam A, Påhlman L, et al. In vitro autoradiography of carcinoembryonic antigen in tissue from patients with colorectal cancer using multifunctional antibody TF2 and (67/68Ga)-labeled haptens by pretargeting. *Am J Nucl Med Mol Imaging.* (2012) 2:141–50.
192. Schoffelen R, van der Graaf WT, Sharkey RM, Franssen GM, McBride WJ, Chang CH, et al. Pretargeted immuno-PET of CEA-expressing intraperitoneal human colonic tumor xenografts: a new sensitive detection method. *EJNMMI Res.* (2012) 2:5. doi: 10.1186/2191-219X-2-5
193. Schoffelen R, Sharkey RM, Goldenberg DM, Franssen G, McBride WJ, Rossi EA, et al. Pretargeted immuno-positron emission tomography imaging of carcinoembryonic antigen-expressing tumors with a bispecific antibody and a 68Ga- and 18F-labeled hapten peptide in mice with human tumor xenografts. *Mol Cancer Ther.* (2010) 9:1019–27. doi: 10.1158/1535-7163.MCT-09-0862
194. Foubert F, Gouard S, Saï-Maurel C, Chérel M, Faivre-Chauvet A, Goldenberg DM, et al. Sensitivity of pretargeted immunoPET using (68)Ga-peptide to detect colonic carcinoma liver metastases in a murine xenograft model: Comparison with (18)FDG PET-CT. *Oncotarget.* (2018) 9:27502–13. doi: 10.18632/oncotarget.25514
195. Touchefeu Y, Bailly C, Frampas E, Eugene T, Rousseau C, Bourgeois M, et al. Promising clinical performance of pretargeted immuno-PET with anti-CEA bispecific antibody and gallium-68-labelled IMP-288 peptide for imaging colorectal cancer metastases: a pilot study. *Eur J Nucl Med Mol Imaging.* (2021) 48:874–82. doi: 10.1007/s00259-020-04989-3
196. Yeku OO, Rao TD, Laster I, Kononenko A, Purdon TJ, Wang P, et al. Bispecific T-Cell engaging antibodies against MUC16 demonstrate efficacy against ovarian cancer in monotherapy and in combination with PD-1 and VEGF inhibition. *Front Immunol.* (2021) 12:663379. doi: 10.3389/fimmu.2021.663379
197. Moek KL, Waaijer SJH, Kok IC, Suurs FV, Brouwers AH. Menke-van der Houven van Oordt CW, et al. (89)Zr-labeled bispecific T-cell engager AMG 211 PET shows AMG 211 accumulation in Cd3-rich tissues and clear, heterogeneous tumor uptake. *Clin Cancer Res.* (2019) 25:3517–27. doi: 10.1158/1078-0432.CCR-18-2918
198. van Brummelen EMJ, Huisman MC. de Wit-van der Veen LJ, Nayak TK, Stokkel MPM, Mulder ER, et al. *(*89)Zr-labeled CEA-targeted IL-2 variant immunocytokine in patients with solid tumors: CEA-mediated tumor accumulation and role of IL-2 receptor-binding. *Oncotarget.* (2018) 9:24737–49. doi: 10.18632/oncotarget.25343
199. Carrasquillo JA, Pandit-Taskar N, O'Donoghue JA, Humm JL, Zanzonico P, Smith-Jones PM, et al. (124)I-huA33 antibody PET of colorectal cancer. *J Nucl Med.* (2011) 52:1173–80. doi: 10.2967/jnumed.110.086165
200. Zeglis BM, Sevak KK, Reiner T, Mohindra P, Carlin SD, Zanzonico P, et al. A pretargeted PET imaging strategy based on bioorthogonal diels-alder click chemistry. *J Nucl Med.* (2013) 54:1389–96. doi: 10.2967/jnumed.112.115840
201. Zeglis BM, Brand C, Abdel-Atti D, Carnazza KE, Cook BE, Carlin S, et al. Optimization of a pretargeted strategy for the PET imaging of colorectal carcinoma via the modulation of radioligand pharmacokinetics. *Mol Pharm.* (2015) 12:3575–87. doi: 10.1021/acs.molpharmaceut.5b00294
202. Vugts DJ, Heuveling DA, Stigter-van Walsum M, Weigand S, Bergstrom M, van Dongen GA, et al. Preclinical evaluation of 89Zr-labeled anti-CD44 monoclonal antibody RG7356 in mice and cynomolgus monkeys: Prelude to Phase 1 clinical studies. *MAbs.* (2014) 6:567–75. doi: 10.4161/mabs.27415
203. Park JW, Jung KH, Lee JH, Moon SH, Cho YS, Lee KH. (89)Zr anti-CD44 immuno-PET monitors CD44 expression on splenic myeloid cells and HT29 colon cancer cells. *Sci Rep.* (2021) 11:3876. doi: 10.1038/s41598-021-83496-3
204. Yoon SO, Lee TS, Kim SJ, Jang MH, Kang YJ, Park JH, et al. Construction, affinity maturation, and biological characterization of an anti-tumor-associated glycoprotein-72 humanized antibody. *J Biol Chem.* (2006) 281:6985–92. doi: 10.1074/jbc.M511165200
205. Jung KH, Lee JH, Kim M, Lee EJ, Cho YS, Lee KH. Celecoxib-Induced Modulation of Colon Cancer CD133 Expression Occurs through AKT Inhibition and Is Monitored by (89)Zr Immuno-PET. *Mol Imaging.* (2022) 2022:4906934. doi: 10.1155/2022/4906934
206. Azhdarinia A, Voss J, Ghosh SC, Simien JA, Hernandez Vargas S, Cui J, et al. Evaluation of Anti-LGR5 antibodies by ImmunoPET for imaging colorectal tumors and development of antibody-drug conjugates. *Mol Pharm.* (2018) 15:2448–54. doi: 10.1021/acs.molpharmaceut.8b00275
207. Cepa A, Ráliš J, Marešová L, Kleinová M, Seifert D, Sieglová I, et al. Radiolabeling of the antibody IgG M75 for epitope of human carbonic anhydrase IX by (61)Cu and (64)Cu and its biological testing. *Appl Radiat Isot.* (2019) 143:87–97. doi: 10.1016/j.apradiso.2018.10.021
208. Manafi-Farid R, Harsini S, Saidi B, Ahmadzadehfar H, Herrmann K, Briganti A, et al. Factors predicting biochemical response and survival benefits following radioligand therapy with [(177)Lu]Lu-PSMA in metastatic castrate-resistant prostate cancer: a review. *Eur J Nucl Med Mol Imaging.* (2021) 48:4028–41. doi: 10.1007/s00259-021-05237-y
209. Manafi-Farid R, Ranjbar S, Jamshidi Araghi Z, Pilz J, Schweighofer-Zwink G, Pirich C, et al. Molecular imaging in primary staging of prostate cancer patients: current aspects and future trends. *Cancers (Basel).* (2021) 13:21. doi: 10.3390/cancers13215360
210. Mease RC, Foss CA, Pomper MG, PET. imaging in prostate cancer: focus on prostate-specific membrane antigen. *Curr Top Med Chem.* (2013) 13:951–62. doi: 10.2174/1568026611313080008
211. Rosenthal SA, Haseman MK, Polascik TJ. Utility of capromab pendetide (ProstaScint) imaging in the management of prostate cancer. *Tech Urol.* (2001) 7:27–37.
212. Petronis JD, Regan F, Lin K. Indium-111 capromab pendetide (ProstaScint) imaging to detect recurrent and metastatic prostate cancer. *Clin Nucl Med.* (1998) 23:672–7. doi: 10.1097/00003072-199810000-00005
213. Akhtar NH, Pail O, Saran A, Tyrell L, Tagawa ST. Prostate-specific membrane antigen-based therapeutics. *Adv Urol.* (2011) 2012:973820. doi: 10.1155/2012/973820
214. Fung EK, Cheal SM, Fareedy SB, Punzalan B, Beylergil V, Amir J, et al. Targeting of radiolabeled J591 antibody to PSMA-expressing tumors: optimization of imaging and therapy based on non-linear compartmental modeling. *EJNMMI Res.* (2016) 6:7. doi: 10.1186/s13550-016-0164-0
215. Pandit-Taskar N, O'Donoghue JA, Morris MJ, Wills EA, Schwartz LH, Gonen M, et al. Antibody mass escalation study in patients with castration-resistant prostate cancer using 111In-J591: lesion detectability and dosimetric projections for 90Y radioimmunotherapy. *J Nucl Med.* (2008) 49:1066–74. doi: 10.2967/jnumed.107.049502
216. Vallabhajosula S, Goldsmith SJ, Kostakoglu L, Milowsky MI, Nanus DM, Bander NH. Radioimmunotherapy of prostate cancer using 90Y- and 177Lu-labeled J591 monoclonal antibodies: effect of multiple treatments on myelotoxicity. *Clin Cancer Res.* (2005) 11:7195s-200s. doi: 10.1158/1078-0432.CCR-1004-0023
217. Pandit-Taskar N, O'Donoghue JA, Durack JC, Lyashchenko SK, Cheal SM, Beylergil V, et al. A phase i/ii study for analytic validation of 89Zr-J591 ImmunoPET as a molecular imaging agent for metastatic prostate cancer. *Clin Cancer Res.* (2015) 21:5277–85. doi: 10.1158/1078-0432.CCR-15-0552
218. van Rij CM, Lütje S, Frielink C, Sharkey RM, Goldenberg DM, Franssen GM, et al. Pretargeted immuno-PET and radioimmunotherapy of prostate cancer with an anti-TROP-2 x anti-HSG bispecific antibody. *Eur J Nucl Med Mol Imaging.* (2013) 40:1377–83. doi: 10.1007/s00259-013-2434-7

219. El Fakiri M, Geis NM, Ayada N, Eder M, Eder AC. PSMA-targeting radiopharmaceuticals for prostate cancer therapy: recent developments and future perspectives. *Cancers* (Basel). (2021) 13:16. doi: 10.3390/cancers13163967
220. Viola-Villegas NT, Sevak KK, Carlin SD, Doran MG, Evans HW, Bartlett DW, et al. Noninvasive Imaging of PSMA in prostate tumors with (89)Zr-Labeled huJ591 engineered antibody fragments: the faster alternatives. *Mol Pharm.* (2014) 11:3965–73. doi: 10.1021/mp500164r
221. Pandit-Taskar N, O'Donoghue JA, Ruan S, Lyashchenko SK, Carrasquillo JA, Heller G, et al. First-in-human imaging with 89Zr-Df-IAB2M Anti-PSMA minibody in patients with metastatic prostate cancer: pharmacokinetics, biodistribution, dosimetry, and lesion uptake. *J Nucl Med.* (2016) 57:1858–64. doi: 10.2967/jnumed.116.176206
222. Vlachostergios PJ, Niaz MJ, Thomas C, Christos PJ, Osborne JR, Margolis DJA, et al. Pilot study of the diagnostic utility of (89) Zr-df-IAB2M and (68) Ga-PSMA-11 PET imaging and multiparametric MRI in localized prostate cancer. *Prostate.* (2022) 82:483–92. doi: 10.1002/pros.24294
223. Elsässer-Beile U, Reischl G, Wiehr S, Bühler P, Wolf P, Alt K, et al. PET imaging of prostate cancer xenografts with a highly specific antibody against the prostate-specific membrane antigen. *J Nucl Med.* (2009) 50:606–11. doi: 10.2967/jnumed.108.058487
224. Alt K, Wiehr S, Ehrlichmann W, Reischl G, Wolf P, Pichler BJ, et al. High-resolution animal PET imaging of prostate cancer xenografts with three different 64Cu-labeled antibodies against native cell-adherent PSMA. *Prostate.* (2010) 70:1413–21. doi: 10.1002/pros.21176
225. Frigerio B, Morlino S, Luison E, Seregni E, Lorenzoni A, Satta A, et al. Anti-PSMA (124)I-scFvD2B as a new immuno-PET tool for prostate cancer: preclinical proof of principle. *J Exp Clin Cancer Res.* (2019) 38:326. doi: 10.1186/s13046-019-1325-6
226. Knowles SM, Zettlitz KA, Tavaré R, Rochefort MM, Salazar FB, Stout DB, et al. Quantitative immunoPET of prostate cancer xenografts with 89Zr- and 124I-labeled anti-PSCA A11 minibody. *J Nucl Med.* (2014) 55:452–9. doi: 10.2967/jnumed.113.120873
227. Zettlitz KA, Tsai WK, Knowles SM, Salazar FB, Kobayashi N, Reiter RE, et al. [(89)Zr]A2cDb Immuno-PET of prostate cancer in a human prostate stem cell antigen knock-in (hPSCA KI) syngeneic model. *Mol Imaging Biol.* (2020) 22:367–76. doi: 10.1007/s11307-019-01386-7
228. Leung K. *(124)I-Anti–prostate Stem-Cell Antigen Back-Mutated 2B3 Diabody*. Molecular Imaging and Contrast Agent Database (MICAD) Bethesda (MD): National Center for Biotechnology Information (US). (2004).
229. Zettlitz KA, Tsai WK, Knowles SM, Kobayashi N, Donahue TR, Reiter RE, et al. Dual-modality immuno-PET and near-infrared fluorescence imaging of pancreatic cancer using an anti-prostate stem cell antigen Cys-Diabody. *J Nucl Med.* (2018) 59:1398–405. doi: 10.2967/jnumed.117.207332
230. van Rij CM, Frielink C, Goldenberg DM, Sharkey RM, Franssen GM, Lütje S, et al. Pretargeted immunoPET of prostate cancer with an anti-TROP-2 x anti-HSG bispecific antibody in mice with PC3 xenografts. *Mol Imaging Biol.* (2015) 17:94–101. doi: 10.1007/s11307-014-0772-x
231. Glumac P, LeBeau A. Targeted immunoPET imaging of prostate cancer using a novel CD133 antibody [abstract]. proceedings of the american association for cancer research annual meeting 2019. *Cancer Res.* (2019) 79:Abstract nr 1150. doi: 10.1158/1538-7445.AM2019-1150
232. Glumac PM, Gallant JP, Shapovalova M, Li Y, Murugan P, Gupta S, et al. Exploitation of CD133 for the targeted imaging of lethal prostate cancer. *Clin Cancer Res.* (2020) 26:1054–64. doi: 10.1158/1078-0432.CCR-19-1659
233. Rodriguez EA, Wang Y, Crisp JL, Vera DR, Tsien RY, Ting R. New Dioxaborolane chemistry enables [(18)F]-positron-emitting, fluorescent [(18)F]-multimodality biomolecule generation from the solid phase. *Bioconjug Chem.* (2016) 27:1390–9. doi: 10.1021/acs.bioconjchem.6b00164
234. Hong H, Nayak TR, Shi S, Graves SA, Fliss BC, Barnhart TE, et al. Generation and screening of monoclonal antibodies for immunoPET imaging of IGF1R in prostate cancer. *Mol Pharm.* (2014) 11:3624–30. doi: 10.1021/mp5003637
235. Ulmert D, Evans MJ, Holland JP, Rice SL, Wongvipat J, Pettersson K, et al. Imaging androgen receptor signaling with a radiotracer targeting free prostate-specific antigen. *Cancer Discov.* (2012) 2:320–7. doi: 10.1158/2159-8290.CD-11-0316
236. Guo X, Zhu H, Zhou N, Chen Z, Liu T, Liu F, et al. Noninvasive detection of HER2 expression in gastric cancer by (64)cu-nota-trastuzumab in pdx mouse model and in patients. *Mol Pharm.* (2018) 15:5174–82. doi: 10.1021/acs.molpharmaceut.8b00673
237. Guo X, Zhou N, Chen Z, Liu T, Xu X, Lei X, et al. Construction of (124)I-trastuzumab for noninvasive PET imaging of HER2 expression: from patient-derived xenograft models to gastric cancer patients. *Gastric Cancer.* (2020) 23:614–26. doi: 10.1007/s10120-019-01035-6
238. Pool M, Kol A, de Jong S, de Vries EGE, Lub-de Hooge MN, Terwisscha van Scheltinga AGT. (89)Zr-mAb3481 PET for HER3 tumor status assessment during lapatinib treatment. *MAbs.* (2017) 9:1370–8. doi: 10.1080/19420862.2017.1371382
239. Janjigian YY, Viola-Villegas N, Holland JP, Divilov V, Carlin SD, Gomes-DaGama EM, et al. Monitoring afatinib treatment in HER2-positive gastric cancer with 18F-FDG and 89Zr-trastuzumab PET. *J Nucl Med.* (2013) 54:936–43. doi: 10.2967/jnumed.112.110239
240. Pereira PMR, Sharma SK, Carter LM, Edwards KJ, Pourat J, Ragupathi A, et al. Caveolin-1 mediates cellular distribution of HER2 and affects trastuzumab binding and therapeutic efficacy. *Nat Commun.* (2018) 9:5137. doi: 10.1038/s41467-018-07608-w
241. Pereira PMR, Mandleywala K, Ragupathi A, Carter LM, Goos J, Janjigian YY, et al. Temporal modulation of HER2 membrane availability increases pertuzumab uptake and pretargeted molecular imaging of gastric tumors. *J Nucl Med.* (2019) 60:1569–78. doi: 10.2967/jnumed.119.225813
242. O'Donoghue JA, Lewis JS, Pandit-Taskar N, Fleming SE, Schöder H, Larson SM, et al. Pharmacokinetics, biodistribution, and radiation dosimetry for (89)Zr-trastuzumab in patients with esophagogastric cancer. *J Nucl Med.* (2018) 59:161–6. doi: 10.2967/jnumed.117.194555
243. Sanchez-Vega F, Hechtman JF, Castel P, Ku GY, Tuvy Y, Won H, et al. EGFR and MET amplifications determine response to Her2 inhibition in ERBB2-amplified esophagogastric cancer. *Cancer Discov.* (2019) 9:199–209. doi: 10.1158/2159-8290.CD-18-0598
244. Price EW, Carnazza KE, Carlin SD, Cho A, Edwards KJ, Sevak KK, et al. (89)Zr-DFO-AMG102 Immuno-PET to determine local hepatocyte growth factor protein levels in tumors for enhanced patient selection. *J Nucl Med.* (2017) 58:1386–94. doi: 10.2967/jnumed.116.187310
245. Jagoda EM, Lang L, Bhadrasetty V, Histed S, Williams M, Kramer-Marek G, et al. Immuno-PET of the hepatocyte growth factor receptor Met using the 1-armed antibody onartuzumab. *J Nucl Med.* (2012) 53:1592–600. doi: 10.2967/jnumed.111.102293
246. Xu B, Li X, Yin J, Liang C, Liu L, Qiu Z, et al. Evaluation of 68Ga-labeled MG7 antibody: a targeted probe for PET/CT imaging of gastric cancer. *Sci Rep.* (2015) 5:8626. doi: 10.1038/srep08626
247. Guo DL, Dong M, Wang L, Sun LP, Yuan Y. Expression of gastric cancer-associated MG7 antigen in gastric cancer, precancerous lesions and H. pylori -associated gastric diseases. *World J Gastroenterol.* (2002) 8:1009–13. doi: 10.3748/wjg.v8.i6.1009
248. Fujiwara K, Akiba H, Tsuji AB, Sudo H, Sugyo A, Nagatsu K, et al. 64Cu-labeled minibody D2101 visualizes CDH17-positive gastric cancer xenografts with short waiting time. *Nucl Med Commun.* (2020) 41:688–95. doi: 10.1097/MNM.0000000000001203
249. Lu RC, She B, Gao WT Ji YH, Xu DD, Wang QS, et al. Positron-emission tomography for hepatocellular carcinoma: Current status and future prospects. *World J Gastroenterol.* (2019) 25:4682–95. doi: 10.3748/wjg.v25.i32.4682
250. Sham JG, Kievit FM, Grierson JR, Miyaoka RS, Yeh MM, Zhang M, et al. Glypican-3-targeted 89Zr PET imaging of hepatocellular carcinoma. *J Nucl Med.* (2014) 55:799–804. doi: 10.2967/jnumed.113.132118
251. Natarajan A, Zhang H, Ye W, Huttad L, Tan M, Chua MS, et al. A Humanized Anti-GPC3 antibody for immuno-positron emission tomography imaging of orthotopic mouse model of patient-derived hepatocellular carcinoma xenografts. *Cancers (Basel).* (2021) 13:16. doi: 10.3390/cancers13163977
252. Yang X, Liu H, Sun CK, Natarajan A, Hu X, Wang X, et al. Imaging of hepatocellular carcinoma patient-derived xenografts using 8?Zr-labeled anti-glypican-3 monoclonal antibody. *Biomaterials.* (2014) 35:6964–71. doi: 10.1016/j.biomaterials.2014.04.089
253. Sham JG, Kievit FM, Grierson JR, Chiarelli PA, Miyaoka RS, Zhang M, et al. Glypican-3-targeting F(ab')2 for 89Zr PET of hepatocellular carcinoma. *J Nucl Med.* (2014) 55:2032–7. doi: 10.2967/jnumed.114.145102

254. Hernandez R, Sun H, England CG, Valdovinos HF, Ehlerding EB, Barnhart TE, et al. CD146-targeted immunoPET and NIRF imaging of hepatocellular carcinoma with a dual-labeled monoclonal antibody. *Theranostics.* (2016) 6:1918–33. doi: 10.7150/thno.15568
255. Li S, England CG, Ehlerding EB, Kutyreff CJ, Engle JW, Jiang D, et al. ImmunoPET imaging of CD38 expression in hepatocellular carcinoma using (64)Cu-labeled daratumumab. *Am J Transl Res.* (2019) 11:6007–15.
256. Jayaprakasam VS, Yeh R, Ku GY, Petkovska I, Fuqua JL, 3rd, et al. Role of imaging in esophageal cancer management in 2020: update for radiologists. *AJR Am J Roentgenol.* (2020) 215:1072–84. doi: 10.2214/AJR.20.22791
257. Hwang YH, Jeong IH, Kang JH, Lee YJ, Kim KI, Lee TS. "Therapeutic Response Monitoring of anti-HER1 therapy with PET imaging biomarkers in Esophageal Squamous Cell Carcinoma Model [Abstract]," in Proceedings of the KNS 2018 Spring Meeting; May 17-18; Korea, Republic of: KNS2018 (2018).
258. Lee TS, Song IH, Shin JI, Park YS, Kim JY, Kim KI, et al. PET Imaging Biomarkers of Anti-EGFR Immunotherapy in Esophageal Squamous Cell Carcinoma Models. Cells. (2018) 7(11). doi: 10.3390/cells7110187
259. Arjaans M, Oude Munnink TH, Oosting SF. Terwisscha van Scheltinga AG, Gietema JA, Garbacik ET, et al. Bevacizumab-induced normalization of blood vessels in tumors hampers antibody uptake. *Cancer Res.* (2013) 73:3347–55. doi: 10.1158/0008-5472.CAN-12-3518
260. Spiegelberg D, Mortensen AC, Selvaraju RK, Eriksson O, Stenerlöw B, Nestor M. Molecular imaging of EGFR and CD44v6 for prediction and response monitoring of HSP90 inhibition in an in vivo squamous cell carcinoma model. *Eur J Nucl Med Mol Imaging.* (2016) 43:974–82. doi: 10.1007/s00259-015-3260-x
261. Wu J, Yuan Y, Tao X-F. Targeted molecular imaging of head and neck squamous cell carcinoma: a window into precision medicine. *Chin Med J (Engl).* (2020) 133:1325–36. doi: 10.1097/CM9.0000000000000751
262. Strome AL, Zhang X, Strome SE. The evolving role of immuno-oncology for the treatment of head and neck cancer. *Laryngoscope Investig Otolaryngol.* (2019) 4:62–9. doi: 10.1002/lio2.235
263. van Dijk LK, Boerman OC, Kaanders JH, Bussink J, PET. Imaging in head and neck cancer patients to monitor treatment response: a future role for EGFR-targeted imaging. *Clin Cancer Res.* (2015) 21:3602–9. doi: 10.1158/1078-0432.CCR-15-0348
264. Song IH, Noh Y, Kwon J, Jung JH, Lee BC, Kim KI, et al. Immuno-PET imaging based radioimmunotherapy in head and neck squamous cell carcinoma model. *Oncotarget.* (2017) 8:92090–105. doi: 10.18632/oncotarget.20760
265. Ku A, Kondo M, Cai Z, Meens J, Li MR, Ailles L, et al. Dose predictions for [(177)Lu]Lu-DOTA-panitumumab F(ab')(2) in NRG mice with HNSCC patient-derived tumour xenografts based on [(64)Cu]Cu-DOTA-panitumumab F(ab')(2) - implications for a PET theranostic strategy. *EJNMMI Radiopharm Chem.* (2021) 6:25. doi: 10.1186/s41181-021-00140-1
266. Benedetto R, Massicano AVF, Crenshaw BK, Oliveira R, Reis RM, Araújo EB, et al. (89)Zr-DFO-cetuximab as a molecular imaging agent to identify cetuximab resistance in head and neck squamous cell carcinoma. *Cancer Biother Radiopharm.* (2019) 34:288–96. doi: 10.1089/cbr.2018.2616
267. van Dijk LK, Yim CB, Franssen GM, Kaanders JH, Rajander J, Solin O, et al. PET of EGFR with (64) Cu-cetuximab-F(ab')2 in mice with head and neck squamous cell carcinoma xenografts. *Contrast Media Mol Imaging.* (2016) 11:65–70. doi: 10.1002/cmmi.1659
268. Even AJ, Hamming-Vrieze O, van Elmpt W, Winnepenninckx VJ, Heukelom J, Tesselaar ME, et al. Quantitative assessment of Zirconium-89 labeled cetuximab using PET/CT imaging in patients with advanced head and neck cancer: a theragnostic approach. *Oncotarget.* (2017) 8:3870–80. doi: 10.18632/oncotarget.13910
269. Burley TA, Da Pieve C, Martins CD, Ciobota DM, Allott L, Oyen WJG, et al. Affibody-Based PET imaging to guide EGFR-targeted cancer therapy in head and neck squamous cell cancer models. *J Nucl Med.* (2019) 60:353–61. doi: 10.2967/jnumed.118.216069
270. Haylock AK, Spiegelberg D, Nilvebrant J, Sandström K, Nestor M. In vivo characterization of the novel CD44v6-targeting Fab fragment AbD15179 for molecular imaging of squamous cell carcinoma: a dual-isotope study. *EJNMMI Res.* (2014) 4:11. doi: 10.1186/2191-219X-4-11
271. Haylock AK, Spiegelberg D, Mortensen AC, Selvaraju RK, Nilvebrant J, Eriksson O, et al. Evaluation of a novel type of imaging probe based on a recombinant bivalent mini-antibody construct for detection of CD44v6-expressing squamous cell carcinoma. *Int J Oncol.* (2016) 48:461–70. doi: 10.3892/ijo.2015.3290
272. Haylock A-K, Nilvebrant J, Mortensen A, Velikyan I, Nestor M, Falk R. Generation and evaluation of antibody agents for molecular imaging of CD44v6-expressing cancers. *Oncotarget.* (2017) 8:65152–70. doi: 10.18632/oncotarget.17996
273. Börjesson PK, Jauw YW, Boellaard R, de Bree R, Comans EF, Roos JC, et al. Performance of immuno-positron emission tomography with zirconium-89-labeled chimeric monoclonal antibody U36 in the detection of lymph node metastases in head and neck cancer patients. *Clin Cancer Res.* (2006) 12:2133–40. doi: 10.1158/1078-0432.CCR-05-2137
274. Jin Y, Liu B, Younis MH, Huang G, Liu J, Cai W, et al. Next-generation molecular imaging of thyroid cancer. *Cancers (Basel).* (2021) 13:213. doi: 10.3390/cancers13133188
275. Liu H, Wang X, Yang R, Zeng W, Peng D, Li J, et al. Recent development of nuclear molecular imaging in thyroid cancer. *Biomed Res Int.* (2018) 2018:2149532. doi: 10.1155/2018/2149532
276. Wagner M, Wuest M, Hamann I, Lopez-Campistrous A, McMullen TPW, Wuest F. Molecular imaging of platelet-derived growth factor receptor-alpha (PDGFRα) in papillary thyroid cancer using immuno-PET. *Nucl Med Biol.* (2018) 58:51–8. doi: 10.1016/j.nucmedbio.2017.12.005
277. D'Alessandria C, Braesch-Andersen S, Bejo K, Reder S, Blechert B, Schwaiger M, et al. Noninvasive In Vivo Imaging and Biologic Characterization of Thyroid Tumors by ImmunoPET Targeting of Galectin-3. *Cancer Res.* (2016) 76:3583–92. doi: 10.1158/0008-5472.CAN-15-3046
278. De Rose F, Braeuer M, Braesch-Andersen S, Otto AM, Steiger K, Reder S, et al. Galectin-3 targeting in thyroid orthotopic tumors opens new ways to characterize thyroid cancer. *J Nucl Med.* (2019) 60:770–6. doi: 10.2967/jnumed.118.219105
279. Peplau E, De Rose F, Reder S, Mittelhäuser M, Scafetta G, Schwaiger M, et al. Development of a chimeric antigen-binding fragment directed against human galectin-3 and validation as an immuno-positron emission tomography tracer for the sensitive in vivo imaging of thyroid cancer. *Thyroid.* (2020) 30:1314–26. doi: 10.1089/thy.2019.0670
280. Peplau E, De Rose F, Eichinger A, Reder S, Mittelhäuser M, Scafetta G, et al. Effective rational humanization of a PASylated anti-galectin-3 Fab for the sensitive PET imaging of thyroid cancer in vivo. *Sci Rep.* (2021) 11:7358. doi: 10.1038/s41598-021-86641-0
281. Bartolazzi A, D'Alessandria C, Parisella MG, Signore A, Del Prete F, Lavra L, et al. Thyroid cancer imaging in vivo by targeting the anti-apoptotic molecule galectin-3. *PLoS One.* (2008) 3:e3768. doi: 10.1371/journal.pone.0003768
282. Wei W, Jiang D, Rosenkrans ZT, Barnhart TE, Engle JW, Luo Q, et al. HER2-targeted multimodal imaging of anaplastic thyroid cancer. *Am J Cancer Res.* (2019) 9:2413–27.
283. Wei W, Liu Q, Jiang D, Zhao H, Kutyreff CJ, Engle JW, et al. Tissue factor-targeted immunopet imaging and radioimmunotherapy of anaplastic thyroid cancer. *Adv Sci (Weinh).* (2020) 7:1903595. doi: 10.1002/advs.201903595
284. Fortin MA, Salnikov AV, Nestor M, Heldin NE, Rubin K, Lundqvist H. Immuno-PET of undifferentiated thyroid carcinoma with radioiodine-labelled antibody cMAb U36: application to antibody tumour uptake studies. *Eur J Nucl Med Mol Imaging.* (2007) 34:1376–87. doi: 10.1007/s00259-006-0346-5
285. Bodet-Milin C, Faivre-Chauvet A, Carlier T, Rauscher A, Bourgeois M, Cerato E, et al. Immuno-PET using anticarcinoembryonic antigen bispecific antibody and 68ga-labeled peptide in metastatic medullary thyroid carcinoma: clinical optimization of the pretargeting parameters in a first-in-human trial. *J Nucl Med.* (2016) 57:1505–11. doi: 10.2967/jnumed.116.172221
286. Bodet-Milin C, Faivre-Chauvet A, Carlier T, Ansquer C, Rauscher A, Frampas E, et al. Anti-CEA Pretargeted Immuno-PET shows higher sensitivity than DOPA PET/CT in detecting relapsing metastatic medullary thyroid carcinoma: post hoc analysis of the iPET-MTC study. *J Nucl Med.* (2021) 62:1221–7. doi: 10.2967/jnumed.120.252791
287. Tummers WS, Willmann JK, Bonsing BA, Vahrmeijer AL, Gambhir SS, Swijnenburg RJ. Advances in diagnostic and intraoperative

molecular imaging of pancreatic cancer. *Pancreas.* (2018) 47:675–89. doi: 10.1097/MPA.0000000000001075
288. González-Gómez R, Pazo-Cid RA, Sarría L, Morcillo M, Schuhmacher AJ. Diagnosis of Pancreatic Ductal Adenocarcinoma by Immuno-Positron Emission Tomography. *J Clin Med.* (2021) 10:6. doi: 10.3390/jcm10061151
289. Makovitzky J. The distribution and localization of the monoclonal antibody-defined antigen 19-9 (CA19-9) in chronic pancreatitis and pancreatic carcinoma. An immunohistochemical study Virchows Arch B Cell. *Pathol Incl Mol Pathol.* (1986) 51:535–44. doi: 10.1007/BF02899058
290. Sawada R, Sun SM, Wu X, Hong F, Ragupathi G, Livingston PO. et al. Human monoclonal antibodies to sialyl-Lewis (CA199) with potent CDC, ADCC, and antitumor activity. *Clin Cancer Res.* (2011) 17:1024–32. doi: 10.1158/1078-0432.CCR-10-2640
291. Viola-Villegas NT, Rice SL, Carlin S, Wu X, Evans MJ, Sevak KK. et al. Applying PET to broaden the diagnostic utility of the clinically validated CA199 serum biomarker for oncology. *J Nucl Med.* (2013) 54:1876–82. doi: 10.2967/jnumed.113.119867
292. Houghton JL, Zeglis BM, Abdel-Atti D, Aggeler R, Sawada R, Agnew BJ. et al. Site-specifically labeled CA199-targeted immunoconjugates for the PET, NIRF, and multimodal PET/NIRF imaging of pancreatic cancer. *Proc Natl Acad Sci U S A.* (2015) 112:15850–5. doi: 10.1073/pnas.1506542112
293. Houghton JL, Abdel-Atti D, Scholz WW. Lewis JS. Preloading with unlabeled ca199 targeted human monoclonal antibody leads to improved PET imaging with (89)Zr-5B1. *Mol Pharm.* (2017) 14:908–15. doi: 10.1021/acs.molpharmaceut.6b01130
294. Houghton JL, Zeglis BM, Abdel-Atti D, Sawada R, Scholz WW, Lewis JS. Pretargeted immuno-PET of pancreatic cancer: overcoming circulating antigen and internalized antibody to reduce radiation doses. *J Nucl Med.* (2016) 57:453–9. doi: 10.2967/jnumed.115.163824
295. Sobol NB, Korsen JA, Younes A, Edwards KJ, Lewis JS. ImmunoPET imaging of pancreatic tumors with (89)zr-labeled gold nanoparticle-antibody conjugates. *Mol Imaging Biol.* (2021) 23:84–94. doi: 10.1007/s11307-020-01535-3
296. Lohrmann C, O'Reilly EM, O'Donoghue JA, Pandit-Taskar N, Carrasquillo JA, Lyashchenko SK, et al. Retooling a blood-based biomarker: phase i assessment of the high-affinity CA19-9 antibody HuMab-5B1 for immuno-PET Imaging of pancreatic cancer. *Clin Cancer Res.* (2019) 25:7014–23. doi: 10.1158/1078-0432.CCR-18-3667
297. Chung YS, Sawada T, Kondo Y, Hirayama K, Inui A, Yamashita Y, et al. Radioimmunodetection with 111In-labeled monoclonal antibody Nd2 in patients with pancreatic cancer. *Jpn J Cancer Res.* (1997) 88:427–34. doi: 10.1111/j.1349-7006.1997.tb00400.x
298. Sharma SK, Wuest M, Way JD, Bouvet VR, Wang M, Wuest FR. Synthesis and pre-clinical evaluation of an (18)F-labeled single-chain antibody fragment for PET imaging of epithelial ovarian cancer. *Am J Nucl Med Mol Imaging.* (2016) 6:185–98.
299. Hull A, Li Y, Bartholomeusz D, Hsieh W, Escarbe S, Ruszkiewicz A, et al. The expression profile and textural characteristics of C595-Reactive MUC1 in pancreatic ductal adenocarcinoma for targeted radionuclide therapy. *Cancers (Basel).* (2020) 13:1. doi: 10.3390/cancers13010061
300. Koivisto L, Bi J, Häkkinen L, Larjava H. Integrin αvβ6: structure, function and role in health and disease. *Int J Biochem Cell Biol.* (2018) 99:186–96. doi: 10.1016/j.biocel.2018.04.013
301. Feng X, Wang Y, Lu D, Xu X, Zhou X, Zhang H, et al. Clinical translation of a (68)Ga-Labeled Integrin α(v)β(6)-targeting cyclic radiotracer for PET imaging of Pancreatic Cancer. *J Nucl Med.* (2020) 61:1461–7. doi: 10.2967/jnumed.119.237347
302. Hausner SH, DiCara D, Marik J, Marshall JF, Sutcliffe JL. Use of a peptide derived from foot-and-mouth disease virus for the noninvasive imaging of human cancer: generation and evaluation of 4-[18F]fluorobenzoyl A20FMDV2 for in vivo imaging of integrin alphavbeta6 expression with positron emission tomography. *Cancer Res.* (2007) 67:7833–40. doi: 10.1158/0008-5472.CAN-07-1026
303. Keat N, Kenny J, Chen K, Onega M, Garman N, Slack RJ, et al. A Microdose PET study of the safety, immunogenicity, biodistribution, and radiation dosimetry of (18)F-FB-A20FMDV2 for imaging the integrin α(v)β(6). *J Nucl Med Technol.* (2018) 46:136–43. doi: 10.2967/jnmt.117.203547
304. Nakamoto R, Ferri V, Duan H, Hatami N, Goel M, Rosenberg J, et al. Pilot-phase PET/CT study targeting integrin α(v)β(6) in pancreatic cancer patients using the cystine-knot peptide-based (18)F-FP-R(0)1-MG-F2. *Eur J Nucl Med Mol Imaging.* (2021). doi: 10.1007/s00259-021-05595-7
305. Hong H, Zhang Y, Nayak TR, Engle JW, Wong HC, Liu B, et al. Immuno-PET of tissue factor in pancreatic cancer. *J Nucl Med.* (2012) 53:1748–54. doi: 10.2967/jnumed.112.105460
306. Luo H, England CG, Shi S, Graves SA, Hernandez R, Liu B, et al. Dual Targeting of Tissue Factor and CD105 for Preclinical PET Imaging of Pancreatic Cancer. *Clin Cancer Res.* (2016) 22:3821–30. doi: 10.1158/1078-0432.CCR-15-2054
307. Luo H, England CG, Goel S, Graves SA Ai F, Liu B, et al. ImmunoPET and near-infrared fluorescence imaging of pancreatic cancer with a dual-labeled bispecific antibody fragment. *Mol Pharm.* (2017) 14:1646–55. doi: 10.1021/acs.molpharmaceut.6b01123
308. Terwisscha van Scheltinga AG, Ogasawara A, Pacheco G, Vanderbilt AN, Tinianow JN, Gupta N, et al. Preclinical Efficacy of an Antibody-Drug Conjugate Targeting Mesothelin Correlates with Quantitative 89Zr-ImmunoPET. *Mol Cancer Ther.* (2017) 16:134–42. doi: 10.1158/1535-7163.MCT-16-0449
309. Lamberts LE. Menke-van der Houven van Oordt CW, ter Weele EJ, Bensch F, Smeenk MM, Voortman J, et al. ImmunoPET with anti-mesothelin antibody in patients with pancreatic and ovarian cancer before anti-mesothelin antibody-drug conjugate treatment. *Clin Cancer Res.* (2016) 22:1642–52. doi: 10.1158/1078-0432.CCR-15-1272
310. England CG, Kamkaew A, Im HJ, Valdovinos HF, Sun H, Hernandez R, et al. ImmunoPET imaging of insulin-like growth factor 1 receptor in a subcutaneous mouse model of pancreatic cancer. *Mol Pharm.* (2016) 13:1958–66. doi: 10.1021/acs.molpharmaceut.6b00132
311. Yoshii Y, Tashima H, Iwao Y, Yoshida E, Wakizaka H, Akamatsu G, et al. Immuno-OpenPET: a novel approach for early diagnosis and image-guided surgery for small resectable pancreatic cancer. *Sci Rep.* (2020) 10:4143. doi: 10.1038/s41598-020-61056-5
312. Boyle AJ, Cao PJ, Hedley DW, Sidhu SS, Winnik MA, Reilly RM. MicroPET/CT imaging of patient-derived pancreatic cancer xenografts implanted subcutaneously or orthotopically in NOD-scid mice using (64)Cu-NOTA-panitumumab F(ab')2 fragments. *Nucl Med Biol.* (2015) 42:71–7. doi: 10.1016/j.nucmedbio.2014.10.009
313. Lepin EJ, Leyton JV, Zhou Y, Olafsen T, Salazar FB, McCabe KE, et al. An affinity matured minibody for PET imaging of prostate stem cell antigen (PSCA)-expressing tumors. *Eur J Nucl Med Mol Imaging.* (2010) 37:1529–38. doi: 10.1007/s00259-010-1433-1
314. Chen W, Li M, Younis MH, Barnhart TE, Jiang D, Sun T, et al. ImmunoPET of trophoblast cell-surface antigen 2 (Trop-2) expression in pancreatic cancer. *Eur J Nucl Med Mol Imaging.* (2022) 49:861–70. doi: 10.1007/s00259-021-05563-1
315. Girgis MD, Olafsen T, Kenanova V, McCabe KE, Wu AM, Tomlinson JS. Targeting CEA in Pancreas Cancer Xenografts with a Mutated scFv-Fc Antibody Fragment. *EJNMMI Res.* (2011) 1:24. doi: 10.1186/2191-219X-1-24
316. Niu G, Murad YM, Gao H, Hu S, Guo N, Jacobson O, et al. Molecular targeting of CEACAM6 using antibody probes of different sizes. *J Control Release.* (2012) 161:18–24. doi: 10.1016/j.jconrel.2012.04.043
317. Li M, Wei W, Barnhart TE, Jiang D, Cao T, Fan K, et al. ImmunoPET/NIRF/Cerenkov multimodality imaging of ICAM-1 in pancreatic ductal adenocarcinoma. *Eur J Nucl Med Mol Imaging.* (2021) 48:2737–48. doi: 10.1007/s00259-021-05216-3
318. Escorcia FE, Houghton JL, Abdel-Atti D, Pereira PR, Cho A, Gutsche NT, et al. ImmunoPET predicts response to met-targeted radioligand therapy in models of pancreatic cancer resistant to met kinase inhibitors. *Theranostics.* (2020) 10:151–65. doi: 10.7150/thno.37098
319. Kim HY, Wang X, Kang R, Tang D, Boone BA, Zeh HJ. 3rd, et al. RAGE-specific single chain Fv for PET imaging of pancreatic cancer. *PLoS One.* (2018) 13:e0192821. doi: 10.1371/journal.pone.0192821
320. van Oostenbrugge T, Mulders P. Targeted PET/CT imaging for clear cell renal cell carcinoma with radiolabeled antibodies: recent developments using girentuximab. *Curr Opin Urol.* (2021) 31:249–54. doi: 10.1097/MOU.0000000000000872

321. Brouwers A, Verel I, Van Eerd J, Visser G, Steffens M, Oosterwijk E, et al. PET radioimmunoscintigraphy of renal cell cancer using 89Zr-labeled cG250 monoclonal antibody in nude rats. *Cancer Biother Radiopharm.* (2004) 19:155–63. doi: 10.1089/108497804323071922
322. Pryma DA, O'Donoghue JA, Humm JL, Jungbluth AA, Old LJ, Larson SM, et al. Correlation of in vivo and in vitro measures of carbonic anhydrase IX antigen expression in renal masses using antibody 124I-cG250. *J Nucl Med.* (2011) 52:535–40. doi: 10.2967/jnumed.110.083295
323. Oosterwijk E, Bander NH, Divgi CR, Welt S, Wakka JC, Finn RD, et al. Antibody localization in human renal cell carcinoma: a phase I study of monoclonal antibody G250. *J Clin Oncol.* (1993) 11:738–50. doi: 10.1200/JCO.1993.11.4.738
324. Smaldone MC, Chen DY Yu JQ, Plimack ER. Potential role of (124)I-girentuximab in the presurgical diagnosis of clear-cell renal cell cancer. *Biologics.* (2012) 6:395–407. doi: 10.2147/BTT.S30413
325. Khandani AH, Rathmell WK, Wallen EM, Ivanovic M. PET/CT with (124)I-cG250: great potential and some open questions. *AJR Am J Roentgenol.* (2014) 203:261–2. doi: 10.2214/AJR.14.12490
326. Stillebroer AB, Franssen GM, Mulders PF, Oyen WJ, van Dongen GA, Laverman P, et al. ImmunoPET imaging of renal cell carcinoma with (124)I- and (89)Zr-labeled anti-CAIX monoclonal antibody cG250 in mice. *Cancer Biother Radiopharm.* (2013) 28:510–5. doi: 10.1089/cbr.2013.1487
327. Cheal SM, Punzalan B, Doran MG, Evans MJ, Osborne JR, Lewis JS, et al. Pairwise comparison of 89Zr- and 124I-labeled cG250 based on positron emission tomography imaging and nonlinear immunokinetic modeling: in vivo carbonic anhydrase IX receptor binding and internalization in mouse xenografts of clear-cell renal cell carcinoma. *Eur J Nucl Med Mol Imaging.* (2014) 41:985–94. doi: 10.1007/s00259-013-2679-1
328. Hekman MCH, Rijpkema M, Aarntzen EH, Mulder SF, Langenhuijsen JF, Oosterwijk E, et al. Positron emission tomography/computed tomography with (89)Zr-girentuximab can aid in diagnostic dilemmas of clear cell renal cell carcinoma suspicion. *Eur Urol.* (2018) 74:257–60. doi: 10.1016/j.eururo.2018.04.026
329. Verhoeff SR, van Es SC, Boon E, van Helden E, Angus L, Elias SG, et al. Lesion detection by [(89)Zr]Zr-DFO-girentuximab and [(18)F]FDG-PET/CT in patients with newly diagnosed metastatic renal cell carcinoma. *Eur J Nucl Med Mol Imaging.* (2019) 46:1931–9. doi: 10.1007/s00259-019-04358-9
330. Oosting SF, Brouwers AH, van Es SC, Nagengast WB, Oude Munnink TH. Lub-de Hooge MN, et al. 89Zr-bevacizumab PET visualizes heterogeneous tracer accumulation in tumor lesions of renal cell carcinoma patients and differential effects of antiangiogenic treatment. *J Nucl Med.* (2015) 56:63–9. doi: 10.2967/jnumed.114.144840
331. Merkx RIJ, Lobeek D, Konijnenberg M, Jiménez-Franco LD, Kluge A, Oosterwijk E, et al. Phase I study to assess safety, biodistribution and radiation dosimetry for (89)Zr-girentuximab in patients with renal cell carcinoma. *Eur J Nucl Med Mol Imaging.* (2021) 48:3277–85. doi: 10.1007/s00259-021-05271-w
332. Vento J, Mulgaonkar A, Woolford L, Nham K, Christie A, Bagrodia A, et al. PD-L1 detection using (89)Zr-atezolizumab immuno-PET in renal cell carcinoma tumorgrafts from a patient with favorable nivolumab response. *J Immunother Cancer.* (2019) 7:144. doi: 10.1186/s40425-019-0607-z
333. Chang AJ, Sohn R, Lu ZH, Arbeit JM, Lapi SE. Detection of rapalog-mediated therapeutic response in renal cancer xenografts using 64Cu-bevacizumab immunoPET. *PLoS One.* (2013) 8:e58949. doi: 10.1371/journal.pone.0058949
334. van Es SC, Brouwers AH, Mahesh SVK, Leliveld-Kors AM, de Jong IJ. Lub-de Hooge MN, et al. *(*89)Zr-Bevacizumab PET: potential early indicator of everolimus efficacy in patients with metastatic renal cell carcinoma. *J Nucl Med.* (2017) 58:905–10. doi: 10.2967/jnumed.116.183475
335. Rosenblum MG, Murray JL, Haynie TP, Glenn HJ, Jahns MF, Benjamin RS, et al. Pharmacokinetics of 111In-labeled anti-p97 monoclonal antibody in patients with metastatic malignant melanoma. *Cancer Res.* (1985) 45:2382–6.
336. Halpern SE, Dillman RO, Witztum KF, Shega JF, Hagan PL, Burrows WM. et al. Radioimmunodetection of melanoma utilizing In-111 965 monoclonal antibody: a preliminary report. *Radiology.* (1985) 155:493–9. doi: 10.1148/radiology.155.2.3983401
337. National Comprehensive Cancer Network (NCCN). NCCN Clinical Practice Guidelines in Oncology. Melanoma: Cutaneous. Version 2.2022. (2022). Available online at: https://www.nccn.org/professionals/physician_gls/pdf/cutaneous_melanoma.pdf.
338. Schweighofer-Zwink G, Manafi-Farid R, Kölblinger P, Hehenwarter L, Harsini S, Pirich C, et al. Prognostic value of 2-[(18)F]FDG PET-CT in metastatic melanoma patients receiving immunotherapy. *Eur J Radiol.* (2022) 146:110107. doi: 10.1016/j.ejrad.2021.110107
339. Broos K, Lecocq Q, Raes G, Devoogdt N, Keyaerts M, Breckpot K. Noninvasive imaging of the PD-1: PD-L1 immune checkpoint: Embracing nuclear medicine for the benefit of personalized immunotherapy. *Theranostics.* (2018) 8:3559. doi: 10.7150/thno.24762
340. Natarajan A, Patel CB, Habte F, Gambhir SS. Dosimetry prediction for clinical translation of (64)Cu-pembrolizumab immunopet targeting human pd-1 expression. *Sci Rep.* (2018) 8:633. doi: 10.1038/s41598-017-19123-x
341. Natarajan A, Mayer AT, Xu L, Reeves RE, Gano J, Gambhir SS. Novel Radiotracer for ImmunoPET Imaging of PD-1 checkpoint expression on tumor infiltrating lymphocytes. *Bioconjug Chem.* (2015) 26:2062–9. doi: 10.1021/acs.bioconjchem.5b00318
342. Bansal A, Pandey MK, Barham W, Liu X, Harrington SM, Lucien F, et al. Non-invasive immunoPET imaging of PD-L1 using anti-PD-L1-B11 in breast cancer and melanoma tumor model. *Nucl Med Biol.* (2021) 100:4–11. doi: 10.1016/j.nucmedbio.2021.05.004
343. Natarajan A, Mayer AT, Reeves RE, Nagamine CM, Gambhir SS. Development of Novel immunopet tracers to image human PD-1 checkpoint expression on tumor-infiltrating lymphocytes in a humanized mouse model. *Mol Imaging Biol.* (2017) 19:903–14. doi: 10.1007/s11307-017-1060-3
344. England CG, Ehlerding EB, Hernandez R, Rekoske BT, Graves SA, Sun H, et al. Preclinical pharmacokinetics and biodistribution studies of 89Zr-labeled pembrolizumab. *J Nucl Med.* (2017) 58:162–8. doi: 10.2967/jnumed.116.177857
345. McCracken MN, Vatakis DN, Dixit D, McLaughlin J, Zack JA, Witte ON. Noninvasive detection of tumor-infiltrating T cells by PET reporter imaging. *J Clin Invest.* (2015) 125:1815–26. doi: 10.1172/JCI77326
346. Ingram JR, Blomberg OS, Rashidian M, Ali L, Garforth S, Fedorov E, et al. Anti-CTLA-4 therapy requires an Fc domain for efficacy. *Proc Natl Acad Sci U S A.* (2018) 115:3912–7. doi: 10.1073/pnas.1801524115
347. Kok IC, Hooiveld JS, van de Donk PP, Giesen D, van der Veen EL. Lub-de Hooge MN, et al. (89)Zr-pembrolizumab imaging as a non-invasive approach to assess clinical response to PD-1 blockade in cancer. *Ann Oncol.* (2022) 33:80–8. doi: 10.1016/j.annonc.2021.10.213
348. Kikuchi M, Clump DA, Srivastava RM, Sun L, Zeng D, Diaz-Perez JA, et al. Preclinical immunoPET/CT imaging using Zr-89-labeled anti-PD-L1 monoclonal antibody for assessing radiation-induced PD-L1 upregulation in head and neck cancer and melanoma. *Oncoimmunology.* (2017) 6:e1329071. doi: 10.1080/2162402X.2017.1329071
349. Ehlerding EB, Lee HJ, Barnhart TE, Jiang D, Kang L, McNeel DG, et al. Noninvasive imaging and quantification of radiotherapy-induced pd-l1 upregulation with (89)zr-df-atezolizumab. *Bioconjug Chem.* (2019) 30:1434–41. doi: 10.1021/acs.bioconjchem.9b00178
350. Islam A, Pishesha N, Harmand TJ, Heston H, Woodham AW, Cheloha RW, et al. Converting an anti-mouse CD4 monoclonal antibody into an scfv positron emission tomography imaging agent for longitudinal monitoring of CD4(+) T Cells. *J Immunol.* (2021) 207:1468–77. doi: 10.4049/jimmunol.2100274
351. Agger R, Petersen MS, Petersen CC, Hansen SB, Stødkilde-Jørgensen H, Skands U, et al. T cell homing to tumors detected by 3D-coordinated positron emission tomography and magnetic resonance imaging. *J Immunother.* (2007) 30:29–39. doi: 10.1097/01.cji.0000211326.38149.7e
352. Wei W, Jiang D, Ehlerding EB, Barnhart TE, Yang Y, Engle JW, et al. CD146-targeted multimodal image-guided photoimmunotherapy of melanoma. *Adv Sci (Weinh).* (2019) 6:1801237. doi: 10.1002/advs.201801237
353. Hu K, Shang J, Xie L, Hanyu M, Zhang Y, Yang Z, et al. PET Imaging of VEGFR with a novel (64)Cu-labeled peptide. *ACS omega.* (2020) 5:8508–14. doi: 10.1021/acsomega.9b03953
354. Sharma SK, Nemieboka B, Sala E, Lewis JS, Zeglis BM. Molecular imaging of ovarian cancer. *J Nucl Med.* (2016) 57:827–33. doi: 10.2967/jnumed.115.172023
355. Cho H, Al-Saden N, Lam H, Möbus J, Reilly RM, Winnik MA. A comparison of DFO and DFO* conjugated to trastuzumab-DM1 for complexing (89)Zr

- In vitro stability and in vivo microPET/CT imaging studies in NOD/SCID mice with HER2-positive SK-OV-3 human ovarian cancer xenografts. *Nucl Med Biol.* (2020) 84:11–9. doi: 10.1016/j.nucmedbio.2019.12.009
356. Kristensen LK, Christensen C, Jensen MM, Agnew BJ, Schjöth-Frydendahl C, Kjaer A, et al. Site-specifically labeled (89)Zr-DFO-trastuzumab improves immuno-reactivity and tumor uptake for immuno-PET in a subcutaneous HER2-positive xenograft mouse model. *Theranostics.* (2019) 9:4409–20. doi: 10.7150/thno.32883
357. Zhang J, Zhao X, Wang S, Wang N, Han J, Jia L, et al. Monitoring therapeutic response of human ovarian cancer to trastuzumab by SPECT imaging with (99m)Tc-peptide-Z(HER2:342). *Nucl Med Biol.* (2015) 42:541–6. doi: 10.1016/j.nucmedbio.2015.02.002
358. Xu Y, Wang L, Pan D, Yan J, Wang X, Yang R, et al. Synthesis of a novel (89)Zr-labeled HER2 affibody and its application study in tumor PET imaging. *EJNMMI Res.* (2020) 10:58. doi: 10.1186/s13550-020-00649-7
359. Qi S, Hoppmann S, Xu Y, Cheng Z, PET. Imaging of HER2-Positive Tumors with Cu-64-labeled affibody molecules. *Mol Imaging Biol.* (2019) 21:907–16. doi: 10.1007/s11307-018-01310-5
360. Jiang D, Im HJ, Sun H, Valdovinos HF, England CG, Ehlerding EB, et al. Radiolabeled pertuzumab for imaging of human epidermal growth factor receptor 2 expression in ovarian cancer. *Eur J Nucl Med Mol Imaging.* (2017) 44:1296–305. doi: 10.1007/s00259-017-3663-y
361. Niu G, Li Z, Cao Q, Chen X. Monitoring therapeutic response of human ovarian cancer to 17-DMAG by noninvasive PET imaging with (64)Cu-DOTA-trastuzumab. *Eur J Nucl Med Mol Imaging.* (2009) 36:1510–9. doi: 10.1007/s00259-009-1158-1
362. Oude Munnink TH, Korte MA, Nagengast WB, Timmer-Bosscha H, Schröder CP, Jong JR, et al. (89)Zr-trastuzumab PET visualises HER2 downregulation by the HSP90 inhibitor NVP-AUY922 in a human tumour xenograft. *Eur J Cancer.* (2010) 46:678–84. doi: 10.1016/j.ejca.2009.12.009
363. Lee HJ, Ehlerding EB, Jiang D, Barnhart TE, Cao T, Wei W, et al. Dual-labeled pertuzumab for multimodality image-guided ovarian tumor resection. *Am J Cancer Res.* (2019) 9:1454–68.
364. Nagengast WB, de Korte MA, Oude Munnink TH, Timmer-Bosscha H, den Dunnen WF, Hollema H, et al. 89Zr-bevacizumab PET of early antiangiogenic tumor response to treatment with HSP90 inhibitor NVP-AUY922. *J Nucl Med.* (2010) 51:761–7. doi: 10.2967/jnumed.109.071043
365. van der Bilt AR. Terwisscha van Scheltinga AG, Timmer-Bosscha H, Schröder CP, Pot L, Kosterink JG, et al. Measurement of tumor VEGF-A levels with 89Zr-bevacizumab PET as an early biomarker for the antiangiogenic effect of everolimus treatment in an ovarian cancer xenograft model. *Clin Cancer Res.* (2012) 18:6306–14. doi: 10.1158/1078-0432.CCR-12-0406
366. Nagengast WB. Lub-de Hooge MN, Oosting SF, den Dunnen WF, Warnders FJ, Brouwers AH, et al. VEGF-PET imaging is a noninvasive biomarker showing differential changes in the tumor during sunitinib treatment. *Cancer Res.* (2011) 71:143–53. doi: 10.1158/0008-5472.CAN-10-1088
367. Sharma SK, Wuest M, Wang M, Glubrecht D, Andrais B, Lapi SE, et al. Immuno-PET of epithelial ovarian cancer: harnessing the potential of CA125 for non-invasive imaging. *EJNMMI Res.* (2014) 4:60. doi: 10.1186/s13550-014-0060-4
368. Sharma SK, Sevak KK, Monette S, Carlin SD, Knight JC, Wuest FR, et al. Preclinical 89Zr immuno-PET of high-grade serous ovarian cancer and lymph node metastasis. *J Nucl Med.* (2016) 57:771–6. doi: 10.2967/jnumed.115.167072
369. Nemieboka B, Sharma SK, Rao TD, Edwards KJ, Yan S, Wang P, et al. Radiopharmacologic screening of antibodies to the unshed ectodomain of MUC16 in ovarian cancer identifies a lead candidate for clinical translation. *Nucl Med Biol.* (2020) 86:9–19. doi: 10.1016/j.nucmedbio.2020.04.006
370. Natarajan A, Srinivas SM, Azevedo C, Greene L, Bauchet AL, Jouannot E, et al. Two patient studies of a companion diagnostic immuno-positron emission tomography (PET) tracer for measuring human ca6 expression in cancer for antibody drug conjugate (ADC) therapy. *Mol Imaging.* (2020) 19:1536012120939398. doi: 10.1177/1536012120939398
371. Crawford A, Haber L, Kelly MP, Vazzana K, Canova L, Ram P, et al. A Mucin 16 bispecific T cell-engaging antibody for the treatment of ovarian cancer. *Sci Transl Med.* (2019) 11:497. doi: 10.1126/scitranslmed.aau7534
372. Waaijer SJ, Giesen D, Ishiguro T, Sano Y, Sugaya N, Schröder CP, et al. Preclinical PET imaging of bispecific antibody ERY974 targeting CD3 and glypican 3 reveals that tumor uptake correlates to T cell infiltrate. *J Immunother Cancer.* (2020) 8:e000548. doi: 10.1136/jitc-2020-000548
373. Han Z, Ke M, Liu X, Wang J, Guan Z, Qiao L, et al. Molecular imaging, how close to clinical precision medicine in lung, brain, prostate and breast cancers. *Mol Imaging Biol.* (2022) 24:8–22. doi: 10.1007/s11307-021-01631-y
374. Ruiz-López E, Calatayud-Pérez J, Castells-Yus I, Gimeno-Peribáñez MJ, Mendoza-Calvo N, Morcillo M, et al. Diagnosis of glioblastoma by immuno-positron emission tomography. *Cancers (Basel).* (2021) 14:1. doi: 10.3390/cancers14010074
375. Tran VL, Novell A, Tournier N, Gerstenmayer M, Schweitzer-Chaput A, Mateos C, et al. Impact of blood-brain barrier permeabilization induced by ultrasound associated to microbubbles on the brain delivery and kinetics of cetuximab: An immunoPET study using (89)Zr-cetuximab. *J Control Release.* (2020) 328:304–12. doi: 10.1016/j.jconrel.2020.08.047
376. Lesniak WG, Chu C, Jablonska A, Du Y, Pomper MG, Walczak P, et al. A distinct advantage to intraarterial delivery of (89)Zr-bevacizumab in pet imaging of mice with and without osmotic opening of the blood-brain barrier. *J Nucl Med.* (2019) 60:617–22. doi: 10.2967/jnumed.118.218792
377. Liu HL, Hsu PH, Lin CY, Huang CW, Chai WY, Chu PC, et al. Focused ultrasound enhances central nervous system delivery of bevacizumab for malignant glioma treatment. *Radiology.* (2016) 281:99–108. doi: 10.1148/radiol.2016152444
378. Molotkov A, Doubrovin M, Bhatt N, Hsu FC, Beserra A, Chopra R, et al. 3D optical/CT as a preclinical companion imaging platform for glioblastoma drug development. *Drug Deliv.* (2020) 27:1686–94. doi: 10.1080/10717544.2020.1833381
379. Souweidane MM, Kramer K, Pandit-Taskar N, Zhou Z, Haque S, Zanzonico P, et al. Convection-enhanced delivery for diffuse intrinsic pontine glioma: a single-centre, dose-escalation, phase 1 trial. *Lancet Oncol.* (2018) 19:1040–50. doi: 10.1016/S1470-2045(18)30322-X
380. Jansen MH, Lagerweij T, Sewing AC, Vugts DJ, van Vuurden DG, Molthoff CF, et al. Bevacizumab targeting diffuse intrinsic pontine glioma: results of 89ZR-bevacizumab PET imaging in brain tumor models. *Mol Cancer Ther.* (2016) 15:2166–74. doi: 10.1158/1535-7163.MCT-15-0558
381. Veldhuijzen van Zanten SEM, Sewing ACP, van Lingen A, Hoekstra OS, Wesseling P, Meel MH, et al. Multiregional tumor drug-uptake imaging by pet and microvascular morphology in end-stage diffuse intrinsic pontine glioma. *J Nucl Med.* (2018) 59:612-5. doi: 10.2967/jnumed.117.197897
382. Yang Y, Hernandez R, Rao J, Yin L, Qu Y, Wu J, et al. Targeting CD146 with a 64Cu-labeled antibody enables in vivo immunoPET imaging of high-grade gliomas. *Proc Natl Acad Sci U S A.* (2015) 112:E6525–34. doi: 10.1073/pnas.1502648112
383. Hernandez R, Sun H, England CG, Valdovinos HF, Barnhart TE, Yang Y, et al. ImmunoPET imaging of CD146 expression in malignant brain tumors. *Mol Pharm.* (2016) 13:2563–70. doi: 10.1021/acs.molpharmaceut.6b00372
384. Strand J, Varasteh Z, Eriksson O, Abrahmsen L, Orlova A, Tolmachev V. Gallium-68-labeled affibody molecule for PET imaging of PDGFRβ expression in vivo. *Mol Pharm.* (2014) 11:3957–64. doi: 10.1021/mp500284t
385. Jansen MH. Veldhuijzen van Zanten SEM, van Vuurden DG, Huisman MC, Vugts DJ, Hoekstra OS, et al. Molecular drug imaging: (89)Zr-bevacizumab pet in children with diffuse intrinsic pontine glioma. *J Nucl Med.* (2017) 58:711–6. doi: 10.2967/jnumed.116.180216
386. Nomura N, Pastorino S, Jiang P, Lambert G, Crawford JR, Gymnopoulos M, et al. Prostate specific membrane antigen (PSMA) expression in primary gliomas and breast cancer brain metastases. *Cancer Cell Int.* (2014) 14:26. doi: 10.1186/1475-2867-14-26
387. Matsuda M, Ishikawa E, Yamamoto T, Hatano K, Joraku A, Iizumi Y, et al. Potential use of prostate specific membrane antigen (PSMA) for detecting the tumor neovasculature of brain tumors by PET imaging with (89)Zr-Df-IAB2M anti-PSMA minibody. *J Neurooncol.* (2018) 138:581–9. doi: 10.1007/s11060-018-2825-5
388. Gonzalez-Junca A, Reiners O, Borrero-Garcia LD, Beckford-Vera D, Lazar AA, Chou W, et al. Positron emission tomography imaging of functional transforming growth factor β (TGFβ) Activity and Benefit of TGFβ inhibition in irradiated intracranial tumors. *Int J Radiat Oncol Biol Phys.* (2021) 109:527–39. doi: 10.1016/j.ijrobp.2020.09.043

389. Kasten BB, Houson HA, Coleman JM, Leavenworth JW, Markert JM, Wu AM, et al. Positron emission tomography imaging with (89)Zr-labeled anti-CD8 cys-diabody reveals CD8(+) cell infiltration during oncolytic virus therapy in a glioma murine model. *Sci Rep.* (2021) 11:15384. doi: 10.1038/s41598-021-00042-x
390. Nobashi TW, Mayer AT, Xiao Z, Chan CT, Chaney AM, James ML, et al. Whole-body PET Imaging of T-cell response to glioblastoma. *Clin Cancer Res.* (2021) 27:6445–56. doi: 10.1158/1078-0432.CCR-21-1412
391. Foster A, Nigam S, Tatum DS, Raphael I, Xu J, Kumar R, et al. Novel theranostic agent for PET imaging and targeted radiopharmaceutical therapy of tumour-infiltrating immune cells in glioma. *EBioMedicine.* (2021) 71:103571. doi: 10.1016/j.ebiom.2021.103571
392. Nigam S, McCarl L, Kumar R, Edinger RS, Kurland BF, Anderson CJ, et al. Preclinical immunopet imaging of glioblastoma-infiltrating myeloid cells using zirconium-89 labeled Anti-CD11b antibody. *Mol Imaging Biol.* (2020) 22:685–94. doi: 10.1007/s11307-019-01427-1
393. Sheybani ND, Breza VR, Paul S, McCauley KS, Berr SS, Miller GW, et al. ImmunoPET-informed sequence for focused ultrasound-targeted mCD47 blockade controls glioma. *J Control Release.* (2021) 331:19–29. doi: 10.1016/j.jconrel.2021.01.023
394. Liu Q, Jiang L, Li K, Li H, Lv G, Lin J, et al. Immuno-PET imaging of (68)Ga-labeled nanobody Nb109 for dynamic monitoring the PD-L1 expression in cancers. *Cancer Immunol Immunother.* (2021) 70:1721–33. doi: 10.1007/s00262-020-02818-y
395. Puttick S, Stringer BW, Day BW, Bruce ZC, Ensbey KS, Mardon K, et al. EphA2 as a Diagnostic imaging target in glioblastoma: a positron emission tomography/magnetic resonance imaging study. *Mol Imaging.* (2015) 14:385–99. doi: 10.2310/7290.2015.00008
396. Da Pieve C, Makarem A, Turnock S, Maczynska J, Smith G, Kramer-Marek G. Thiol-Reactive PODS-bearing bifunctional chelators for the development of egfr-targeting [(18)F]AlF-affibody conjugates. *Molecules.* (2020) 25:1562. doi: 10.3390/molecules25071562
397. Lee FT, Burvenich IJ, Guo N, Kocovski P, Tochon-Danguy H, Ackermann U, et al. L-Tyrosine confers residualizing properties to a d-amino acid-rich residualizing peptide for radioiodination of internalizing antibodies. *Mol Imaging.* (2016) 15:1536012116647535. doi: 10.1177/1536012116647535
398. Chakravarty R, Goel S, Valdovinos HF, Hernandez R, Hong H, Nickles RJ, et al. Matching the decay half-life with the biological half-life: ImmunoPET imaging with (44)Sc-labeled cetuximab Fab fragment. *Bioconjug Chem.* (2014) 25:2197–204. doi: 10.1021/bc500415x
399. Tang Y, Hu Y, Liu W, Chen L, Zhao Y, Ma H, et al. A radiopharmaceutical [(89)Zr]Zr-DFO-nimotuzumab for immunoPET with epidermal growth factor receptor expression in vivo. *Nucl Med Biol.* (2019) 70:23–31. doi: 10.1016/j.nucmedbio.2019.01.007
400. Luo H, Hernandez R, Hong H, Graves SA, Yang Y, England CG, et al. Noninvasive brain cancer imaging with a bispecific antibody fragment, generated via click chemistry. *Proc Natl Acad Sci U S A.* (2015) 112:12806–11. doi: 10.1073/pnas.1509667112
401. Gaedicke S, Braun F, Prasad S, Machein M, Firat E, Hettich M, et al. Noninvasive positron emission tomography and fluorescence imaging of CD133+ tumor stem cells. *Proc Natl Acad Sci U S A.* (2014) 111:E692–701. doi: 10.1073/pnas.1314189111
402. Pandya DN, Sinha A, Yuan H, Mutkus L, Stumpf K, Marini FC, et al. Imaging of fibroblast activation protein alpha expression in a preclinical mouse model of glioma using positron emission tomography. *Molecules.* (2020) 25:16. doi: 10.3390/molecules25163672
403. de Lucas AG, Schuhmacher AJ, Oteo M, Romero E, Cámara JA, de Martino A, et al. Targeting MT1-MMP as an immunopet-based strategy for imaging gliomas. *PLoS One.* (2016) 11:e0158634. doi: 10.1371/journal.pone.0158634
404. Escorcia FE, Steckler JM, Abdel-Atti D, Price EW, Carlin SD, Scholz WW, et al. Tumor-Specific Zr-89 Immuno-PET imaging in a human bladder cancer model. *Mol Imaging Biol.* (2018) 20:808–15. doi: 10.1007/s11307-018-1177-z
405. Hoang TT, Mandleywala K, Viray T, Tan KV, Lewis JS, Pereira PMR. EGFR-Targeted ImmunoPET of UMUC3 orthotopic bladder tumors. *Mol Imaging Biol.* (2022). doi: 10.1007/s11307-022-01708-2
406. Beckford Vera DR, Smith CC, Bixby LM, Glatt DM, Dunn SS, Saito R, et al. Immuno-PET imaging of tumor-infiltrating lymphocytes using zirconium-89 radiolabeled anti-CD3 antibody in immune-competent mice bearing syngeneic tumors. *PLoS One.* (2018) 13:e0193832. doi: 10.1371/journal.pone.0193832
407. Lee JH, Kim H, Yao Z, Lee SJ, Szajek LP, Grasso L, et al. Tumor and organ uptake of (64)Cu-labeled MORAb-009 (amatuximab), an anti-mesothelin antibody, by PET imaging and biodistribution studies. *Nucl Med Biol.* (2015) 42:880–6. doi: 10.1016/j.nucmedbio.2015.07.008
408. Chia PL, Parakh S, Tsao MS, Pham NA, Gan HK, Cao D, et al. Targeting and efficacy of novel mab806-antibody-drug conjugates in malignant mesothelioma. *Pharmaceuticals* (Basel). (2020) 13:10. doi: 10.3390/ph13100289
409. Song IH, Lee TS, Hong HH, Kim KI, Lee YJ, Kang JH, et al. 64Cu/177Lu labeled anti L1-CAM antibody for a diagnostic and therapeutic convergence radiopharmaceutical in cholangiocarcinoma. *J Nucl Med.* (2014) 55:172.
410. Lee TS, Jeong MS, Song IH, Hong HH, Kim KI, Lee YJ, et al. Small animal PET imaging of 64Cu-NOTA-chimeric anti-L1 cell adhesion molecule antibody in cholangiocarcinoma xenografted model. *J Nucl Med.* (2013) 54:1159.
411. Carvalho LS, da Silva OB, de Almeida GC, de Oliveira JD, Parachin NS, Carmo TS. *Production Processes for Monoclonal Antibodies*. Jozala AF, editor. London: IntechOpen (2017), p. 182–98.

Conflict of Interest: The authors declare that the research was conducted in the absence of any commercial or financial relationships that could be construed as a potential conflict of interest.

Publisher's Note: All claims expressed in this article are solely those of the authors and do not necessarily represent those of their affiliated organizations, or those of the publisher, the editors and the reviewers. Any product that may be evaluated in this article, or claim that may be made by its manufacturer, is not guaranteed or endorsed by the publisher.

GLOSSARY

[^{18}F]FDG, [^{18}F]FluoroDeoxyGlucose; [^{18}F]FDOPA, [^{18}F]Fluoro-L-Dopa; ACKR3, Atypical Chemokine Receptor 3; ADC, Antibody-Drug Conjugate; ATC, Anaplastic Thyroid Carcinoma; BBB, Blood-Brain Barrier; bsAb, bispecific Antibody; CA 15-3, Cancer Antigen 15-3; CA 19-9, Carbohydrate Antigen 19-9; CA125, Carbohydrate Antigen 125; CA6, Carbonic Anhydrase 6; CA-IX, Carbonic Anhydrase-IX; CD, Clusters of Differentiation; CDCP1, CUB domain-containing protein 1; CEA, Carcinoembryonic Antigen; CH, Constant Heavy Chain; CNS, Central Nervous System; CT, Computed Tomography; CTLA-4, Cytotoxic T-lymphocyte Associated Protein; CXCR, C-X-C Chemokine Receptor; Df, Desferrioxamine; Dll4, Delta-like ligand 4; dsFv, disulfide Fragment variable; ECM, Extracellular Matrix; EGFR, Epidermal Growth Factor Receptor; EphA2, Ephrin Receptor A2; Fab, antigen-binding Fragment; FAP-α, Fibroblast Activation Factor-Alpha; Fc, crystallizable Fragment; Gal-3, β-galactoside-binding protein galectin-3**;** GITR, Glucocorticoid-Induced Tumor Necrosis Factor Receptor; GPC3, Glypican 3; GRP78, Glucose-regulated protein 78; HCC, Hepatocellular Carcinoma; HER, Human Epithelial Growth Factor Receptor **;** HGF, Hepatocyte Growth Factor; HNSCC, Head and Neck Squamous Carcinoma; HSG, Histamine-Succinyl-Glycine; HSP90, Heat Shock Protein 90; ICAM-1, Intercellular Adhesion Molecule-1; ICI, Immune Checkpoint Inhibitor; ICOS, Inducible T-Cell Costimulatory Receptor; IGF-1R, Insulin-like Growth Factor-1 Receptor; IgG, Immunoglobulin G; IHC, Immunohistochemistry; KRAS, Kirsten Rat Sarcoma Virus; LGR5, Leucine-rich repeat-containing G-protein coupled Receptor 5; mAb, monoclonal Antibody; MMP, Matrix metalloproteinase; MRI, Magnetic Resonance Imaging; MSLN, Mesothelin; MTC, Medullary Thyroid Carcinoma; mTOR, Mammalian Target of Rapamycin; MUC, Mucin; NIRF, Near-Infrared Fluorophore; NSCLC, Non-Small Cell Lung Cancer; OX40, Tumor Necrosis Factor (Ligand) Superfamily, Member 4; PD-1/PD-L1, Programmed Cell Death Protein-1/Ligand; PDAC, Pancreatic Ductal AdenoCarcinoma; PDGF/PDGFR, Platelet-Derived Growth Factor/Receptor; PET, Positron Emission Tomography; PSCA, Prostate Stem Cell Antigen; PSMA, Prostate Specific Membrane Antigen; PTC, Papillary Thyroid Carcinoma; RAGE, Receptor for advanced glycation end products; RANK/RANKL, Receptor Activator of Nuclear Factor-Kappa B/Ligand; RCC, Renal Cell Carcinoma; RTK, Receptor Tyrosine Kinase; scdsFv, single-chain disulfide Fragment variable; scFv, single-chain Fragment variable; sdAb, single-domain Antibody; SUV, Standardized Uptake Value; TAG-72, Tumor-Associated Glycoprotein-72; TAM, Tumor-Associated Macrophage; TBR, Target-to-Background Ratio; TF, Tissue factor; TF, Tissue Factor (CD142); TfR, Transferrin receptor; TGF, Transforming Growth Factor; TIL, Tumor Infiltrating Lymphocyte; TIM-3, T-Cell Immunoglobulin and Mucin Domain-Containing-3**;** TNF, Tumor Necrosis Factor; TROP-2, Trophoblast cell-surface antigen-2, known as tumor-associated calcium signal transducer 2; VEGF/VEGFR, Vascular Endothelial-Derived Growth Factor/Receptor.